Received: 18 April 2021 | Accepted: 12 July 2021

DOI: 10.1111/imm.13398

Immunology
The Journal of cells, molecules, systems and technologies
British Society for immunology

ORIGINAL ARTICLE

Critical roles of the E3 ubiquitin ligase FBW7 in B-cell response and the pathogenesis of experimental autoimmune arthritis

Chunlei Feng[1] | **Lingyun Li**[1] | **Lei Zhou**[1] | **Dali Li**[1] | **Mingyao Liu**[1] | **Shuhua Han**[2] | **Biao Zheng**[1,2]

[1]Shanghai Key Laboratory of Regulatory Biology, Institute of Biomedical Sciences and School of Life Sciences, East China Normal University, Shanghai, China

[2]Department of Pathology and Immunology, Baylor College of Medicine, Houston, TX, USA

Correspondence
Biao Zheng, Shanghai Key Laboratory of Regulatory Biology, Institute of Biomedical Sciences and School of Life Sciences, East China Normal University, Shanghai 201203, China.
Email: bzheng@bio.ecnu.edu.cn

Senior author: Chunlei Feng

Funding information
This research did not receive any specific grant from funding agencies in the public, commercial or not-for-profit sectors.

Abstract

Proper regulation of B-cell function is essential for effective humoral immunity and maintenance of immune tolerance. Here, we found that FBW7 (F-box/WD40 repeat-containing protein 7) is highly expressed in germinal centre B and B1 cells, and confirmed that it has an intrinsic role in maintaining homeostasis of mature B cells and B-1 cells. FBW7 deletion led to an impairment of antibody response, and although germinal centre formation was not affected, antibody class-switch recombination and affinity maturation processes were defective. Likewise, memory immune response was severely impaired. Moreover, FBW7 ablation ameliorated the pathogenesis of an autoimmune disease model, collagen-induced arthritis, by reducing the production of anti-collagen II autoantibodies. Taken together, these data suggest that FBW7 may be an attractive target for developing new therapeutics for the treatment of autoimmune diseases.

KEYWORDS

affinity maturation, class switch recombination, collagen-induced arthritis, F-box/WD repeat-containing protein 7, germinal centre B cells, mature B cells

INTRODUCTION

B cells (B2 B cells) arise from hematopoietic stem cells (HSCs) in the bone marrow (BM) and differentiate into progenitor stages with increasingly limited multipotentiality. After pro-/pre-B cells rearrange their immunoglobulin (Ig) heavy and light chain gene segments to produce functional antibody genes, they enter the immature B-cell stage [1, 2]. After selection, they exit the BM into the bloodstream as immature/transitional B cells expressing surface IgM and IgD, and migrate to the peripheral lymphoid organs [3].

Once stimulated by antigens, peripheral mature B cells are activated and differentiate into plasma cells through extra-follicular reaction or initiation of T cell-dependent germinal centre (GC) formation [4–7]. Generally, B-cell subsets are acknowledged to have a specific division of labour in response to T cell-independent (TI) or T cell-dependent (TD)

Abbreviations: AID, activation-induced cytidine deaminase; ASCs, antibody secreting cells; BCRs, B-cell antigen receptors; BM, bone marrow; CB, centroblasts; CC, centrocytes; CIA, collagen-induced arthritis; CSR, class switch recombination; DZ, dark zone; FBW7, F-box/WD40 repeat-containing protein 7; FDCs, follicular dendritic cells; FO, follicular; GC, germinal centre; HSCs, hematopoietic stem cells; Ig, immunoglobulin; LZ, light zone; MZ, Marginal zone; NP-CGG, NP conjugated chicken γ-globulin; RA, rheumatoid arthritis; SHM, somatic hypermutation; Tfh, follicular helper T cells.

antigens. Marginal zone (MZ) and B1 cell subsets are considered the major players in TI immune responses, which serve as the first line of defence by responding rapidly via the extra-follicular response [8–10]. Thereafter, follicular (FO) B cells dominate in more delayed highly specific antibody responses, which are mainly triggered by TD antigens [11]. This latter robust immune response requires the formation of a specialized transient structure, the GC [6, 7, 12, 13]. Upon encountering the TD antigen presented by follicular dendritic cells (FDCs), FO B cells begin to proliferate rapidly in the follicle, generating GCs with the help of follicular helper T cells (Tfh). These proliferating B cells, known as centroblasts, undergo somatic hypermutation (SHM) to generate an expanded repertoire of B-cell antigen receptors (BCRs) with different affinities, constituting the dark zone (DZ) of the GC [7, 14, 15]. Centroblasts express the chemokine receptor CXCR4, which localizes them within the DZ. Later, centroblasts down-regulate the expression of CXCR4 and migrate to an area adjacent to the DZ known as the light zone (LZ) of GCs. The level of CXCR4 plays an important role in the segregation of dark and light zones in GCs. In the LZ, the centroblasts differentiate into centrocytes and undergo Ig class-switching. The class switch recombination (CSR) process allows the production of different Ig classes associated with distinct effector functions. B cells migrate back and forth between the DZ and LZ and undergo clonal expansion and SHM in the DZ followed by BCR affinity-based selection in the LZ. Following iterations of these processes, B cells with lower affinity BCRs undergo apoptosis and only B cells with high affinity BCRs can exit the GC and further differentiate into long-lived antibody secreting cells (ASCs) and memory B cells [6, 7, 12, 13] in the periphery. These effector cells are those that provide protection against a subsequent infection, in some cases mediating lifelong immunity against specific pathogens.

The GC reaction is essential for effective humoral immunity, and its dysregulation may contribute to various diseases, such as cancer, autoimmunity or immunodeficiency [16]. Ectopic GCs can also emerge in non-lymphoid tissues under a variety of inflammatory conditions, including autoimmune diseases [17, 18]. The production of class-switched high-affinity autoantibodies derived from ectopic GCs is a hallmark of many autoimmune inflammatory diseases, including rheumatoid arthritis (RA). Patients with RA or other autoimmune diseases have been successfully treated using B-cell depletion therapies [19–21], demonstrating that the B-cell lineage plays a key role in human autoimmune diseases [22–24]. Correspondingly, GC formation and anti-collagen antibody production are the key pathogenic functions of B cells in the autoimmune collagen-induced arthritis (CIA) model; indeed, GC B cells are a major driver of CIA through the production of anti-CII antibodies [16, 25–28]. Accordingly, we propose that by targeting regulators of the GC reaction, the production of pathogenic autoantibodies could be limited and the inflammatory response alleviated.

FBW7 (F-box and WD repeat domain-containing 7), which is part of the substrate-binding subunit of E3 ubiquitin ligase SCF^{FBW7} (a complex of SKP1, cullin-1 and FBW7), is involved in the ubiquitination and degradation of many substrates [29–31]. It has three isoforms (α, β and γ) generated by alternative splicing, each of which differs in the N-terminal region that specifies its subcellular localization [29, 30]. FBW7 has anti-tumour or pro-survival effects in different types of cancer, depending on the cellular environment and the related substrates degraded in the tumour [29, 30]. In addition to its role in tumours, FBW7 has been reported to function in viral immunity and inflammatory responses [32–36]. Moreover, deletion of FBW7 in hematopoietic stem cells results in impaired self-renewal [37, 38]. Accumulating evidence suggests a key role of FBW7 in lymphocyte function and that it is required for the survival and fitness of mature B cells [39]. In the absence of FBW7, B cells exhibit increased apoptosis and decreased proliferation following BCR ligation [39]. However, the role of FBW7 in the activation and differentiation of mature B cells after stimulation by antigen and its subsequent role in mediating robust antibody responses has not been fully defined, especially in the GC stage of B-cell response.

In the present study, we show that FBW7 is highly expressed in GC B cells and B1 cells. In line with previous findings, it has been found that FBW7 is important for the maintenance of normal mature B and B1 cell populations. To investigate the potential function of FBW7 in GC B cells, we undertook an analysis of immune function following stimulation by TD antigens in mice with deficient FBW7 expression in GC B cells. The results revealed that FBW7 deficiency did not affect GC formation, but that Ig class switching and affinity maturation were severely impaired, leading to a dramatic reduction of the production of class-switched high-affinity antibodies and a defective secondary antibody responses. Furthermore, these FBW7-deficient mice showed delayed onset and reduced severity of collagen-induced arthritis (CIA) as well as a reduced level of anti-collagen II autoantibodies. In summary, our studies demonstrated that FBW7 is an indispensable regulator of B cell homeostasis and the GC reaction, providing a theoretical basis for exploiting FBW7 regulation as a potential target for B cell-driven autoimmune responses.

METHODS

Mice

C57BL/6 mice (6–8 weeks) were purchased from Vital River Laboratory Animal Technology (Beijing, China). $FBW7^{f/f}$ mice on a C57BL/6J background were kindly

provided by Professor Ping Wang (Tongji University Medical School, Shanghai, China). The CD19-Cre and Cγ1-cre C57BL/6J mice were obtained from Jackson Laboratories. $FBW7^{f/f}$ mice were crossed to CD19-Cre mice or Cγ1-Cre mice to generate FBW7-deficient mice at specific B-cell stages. The corresponding littermates ($CD19\text{-}cre^{+/-}$ or $C\gamma1\text{-}cre^{+/-}$) were used as controls. All mice were maintained in specific pathogen-free (SPF) conditions in the animal facility of East China Normal University (Shanghai, China), and all animal experiments conformed to the regulations drafted by the Association for Assessment and Accreditation of Laboratory Animal Care in Shanghai and were approved by the East China Normal University Center for Animal Research (M20150401). Transgenic animals were genotyped by PCR using total DNA from tail biopsies. Male and female mice were used for experiments. Primers are listed in Table S1.

Immunization

For T cell-independent antibody responses, mice aged 7–10 weeks were immunized by intraperitoneal (i.p.) injection of 50 μg NP-Ficoll (Biosearch Technologies, Novato, CA, USA) in PBS. For T cell-dependent antibody responses, mice aged 7–10 weeks were immunized by intraperitoneal (i.p.) injection of 100 μg alum-precipitated NP-CGG (Biosearch Technologies) and analysed 12–13 days later in the primary immunization. Two months later, mice were boosted with 20 μg soluble NP-CGG in PBS (i.p. injected) for secondary immunization.

Flow cytometry analysis

To prepare splenocytes, spleens were taken and cut in half with a razor blade. Typically, one half was used for frozen sections, and the other for enzyme-linked immunospot assay (ELISPOT) and flow cytometry (FCM) analysis. In some experiments, the whole spleen was used for FCM analysis or cell sorting. Single cell suspensions were prepared by passing the spleen through a 70-μM cell strainer (Falcon, Corning, NY, USA). After 5 min of 400 g centrifugation, erythrocytes were depleted by using red cell lysis solution (buffer containing 155 mM NH4Cl, 10 mM KHCO3, 1 mM EDTA). Then cells were washed and suspended in magnetic-activated cell sorting (MACS) buffer (PBS/2% BSA/200 mM EDTA). MACS buffer was used for washing cells between each staining step. Cells were stained with the indicated antibodies for 30 min on ice after blocking FcγR-mediated non-specific binding by incubation with anti-mouse CD16/CD32, according to the manufacturers' suggested protocols. Like splenocytes, bone marrow cells and peritoneal wash cells were stained with antibodies after removal of red blood cells. The flow cytometry staining procedure for cells cultured *in vitro* was the same as that for splenocytes except for the removal of erythrocytes. Cells were collected using a FACScalibur or BD LSRFortessa™ (BD Bioscience, San Diego, CA, USA) flow cytometer, and data were analysed using FlowJo software V10 (Tree Star Inc.). All antibodies are listed in Table S2.

Cell isolation and sorting

For mouse B-cell subsets: MZ B cells ($B220^+CD23^{low/-}CD21^{high}$), FO B cells ($B220^+CD23^+CD21^-$) and naive/mature B cells ($B220^+IgM^{low}IgD^+CD23^+$) were isolated from spleens of unimmunized C57BL/6 mice by fluorescence-activated cell sorting (FACS). Thirteen days after NP-CGG immunization, memory B cells ($B220^+CD138^-CD38^+IgG1^+$) and GC B ($B220^+CD138^-CD38^-IgG1^+$) cells in the spleens of C57BL/6 mice were sorted using a FACS Aria II. The purity of the sorted cells was confirmed by FCM analysis (>95%). All samples were subjected to real-time PCR. Generally, single-cell suspensions were prepared as described above and then labelled with antibodies. *For Human B subsets*: Human tonsils were obtained after routine tonsillectomy at the Sixth People's Hospital of Shanghai. Informed consent was obtained from the patients or there was an exemption from informed consent because residual material after diagnosis was used. All samples were fully anonymized. Tissue collection was approved by the Ethical and Scientific Committees of East China Normal University. Tissues were placed in cold phosphate-buffered saline (PBS) immediately after surgery, as previously described [40]. They were cut into pieces with surgical scissors before mechanical homogenization with a syringe plunger. The cell suspension was then passed through a 70-μm sterile cell strainer to remove debris and aggregated material. Mononuclear cells were isolated using Lymphoprep™ (Stemcell, Vancouver, Canada) density gradient centrifugation at 400 g for 30 min. To shorten the fluorescence-activated cell sorting time, enriched B cells were first obtained by magnetic depletion of non-B cells (T cells, NK cells, monocytes, dendritic cells, etc.), which were labelled with a cocktail of biotinylated CD2, CD14, CD16, CD3 and CD235a (glycophorin A) antibodies and subsequently with streptavidin-conjugated magnetic beads (Miltenyi Biotec, Germany). After consecutive washes with MACS buffer, the cell suspension was passed through a 40-μM sterile cell strainer to remove aggregates and then stained for multiparametric FACS. The B-cell populations were phenotypically defined as naive B cells ($CD19^+IgD^+CD38^-$), pre-GC B cells ($CD19^+IgD^+CD38^+$),

GC B cells ($CD19^+IgD^-CD38^+CD44^-$), memory B cells ($CD19^+IgD^-CD38^-CD44^+$), centroblasts ($CD19^+IgD^-CD38^+CD44^-CXCR4^+$) or centrocytes ($CD19^+IgD^-CD38^+CD44^-CXCR4^-$) and were further sorted using a FACS Aria II (BD Bioscience) to >95% purity. Afterwards, cells were collected into the appropriate medium and kept on ice for subsequent experiments such as real-time PCR or Western blotting. Representative cell sorting strategies are shown in Figure S1. Antibody information is listed in Table S2.

Western blotting

Cells were harvested and lysed for 25 min in 1*RIPA buffer (CST, BSN, USA) containing a protease and phosphatase inhibitor cocktail. The protein concentration of samples was determined using BCA protein assay reagent kits (Beyotime, Shanghai, China) after which 25–50 μg protein was separated by standard SDS-PAGE on 12% or 15% gels and then transferred to PVDF membranes (Bio-Rad, CA, USA). These were subsequently blotted with specific primary antibodies followed by horseradish peroxidase (HRP)-conjugated secondary antibodies and visualized by Super Signal West Pico stable peroxide solution (Thermo Scientific). The antibodies used in this study are listed in Table S2.

Real-time PCR

Total RNA was extracted from the isolated B-cell subsets using RNA extraction kits (Gene Mark biolab, Taiwan, China), and reverse transcription was performed with ReverTra Ace (Toyobo, Osaka, Japan) according to the manufacturer's instructions. To examine the mRNA expression status of the designated genes, cDNA fragments were amplified by Hieff® qPCR SYBR Green Master Mix (YESAN, Shanghai, China). Assays were performed using ABI PRISM 7000 (Applied Biosystems, USA). All reactions were performed in duplicate. The mRNA level of each gene was first normalized to the expression level of β-actin by the $2^{-\Delta\Delta Ct}$ method. To facilitate comparison of the B-cell subsets, naive B cells were used as the control group, against which the data of the other groups were normalized. All data are reported as relative mRNA expression levels. All primer sequences used in this study are listed in Table S1.

In vitro B-cell stimulation

Naive B cells were sorted from unimmunized mouse spleens by magnetic depletion of labelled cells. Cells were labelled with a cocktail of biotin-conjugated antibodies against CD43 (Ly-48), CD4 (L3T4) and Ter-119, followed by streptavidin-coupled magnetic beads (Miltenyi Biotec). Untouched naive B cells ($B220^+$% >95%) were adjusted to a density of 1×10^6/ml and cultured in complete RPMI 1640 medium supplemented with 10% fetal bovine serum (Millipore, Billerica, MA, USA), 100 U/ml penicillin (Gibco, Carlsbad, CA, USA), 100 mg/ml streptomycin (Gibco), 2 mM L-glutamine (Gibco), 1 mM sodium pyruvate (Gibco) and non-essential amino acids solution (Gibco), 10 mm HEPES and 0·05 mM β-mercaptoethanol (Sigma) at 37°C in a humidified atmosphere containing 5% CO_2. For in vitro class-switching assays, cells were stimulated by 20 μg/ml LPS (Sigma) plus 25 ng/ml IL-4 (R&D) for the specific time described in the figure legends. Finally, cells were collected for FCM analysis or Western blotting. For B-cell proliferation assessment, purified naive B cells were first labelled by 2·5 μM 5-(and 6)-carboxyfluorescein diacetate succinimidyl ester (CFSE) (Thermo Fisher Scientific, Ashville NC, USA) for 10 min at 37°C. After washing, the labelled cells were cultured under the specific conditions described above. Eventually, cells were collected and diluted fluorescence peaks of CFSE were analysed by flow cytometry using an Attune NxT Flow Cytometer (Thermo Scientific, USA). Viability of B cells was also measured by flow cytometry using a Zombie Fixable Viability Kit, gating living cells by Zombie-negativity.

ELISA and ELISPOT

Enzyme-linked immunosorbent assays (ELISA) for NP-specific Ig serum concentrations and ELISPOT for NP-specific antibody secreting cells (ASCs) were carried out as described [42, 43]. Blood samples were collected from the eye vein at different time-points, kept at room temperature (RT) for 2 h and centrifuged at 2900×*g* for 10 min, and repeated once. The supernatants were harvested and stored at −80°C before the ELISA. Briefly, 96-well plates (Corning, NY, USA) were coated with 50 μg/ml NP_5-BSA (for high-affinity NP-specific Ig titres) (Biosearch Technologies) or NP_{23}-BSA (for total NP-specific Ig titres) (Biosearch Technologies) in 0·1 M carbonate buffer at 4°C overnight. The plates were then blocked with PBS containing 10% (v/v) bovine serum for 2 h at 37°C. Dilutions of test serum collected at the indicated time-points were added for 2 h at 37°C, followed by detection using anti-IgM or anti-IgG1 coupled to HRP (Southern Biotechnology, Birmingham, AL, USA). 3,3′, 5,5′-tetramethylbenzidine TMB (Abcam, Cambridge, UK) was added subsequently, and the absorbance was measured at 450 nm after stopping the reaction with 1 m H_2SO_4 (Abcam). Each dilution of serum was duplicated. A mixture of sera from naïve C57BL/6J mice was used as a negative control in each plate, and antibody levels were shown as relative titres.

For ELISPOT assays: PVDF membranes were coated with 50 μg/ml NP_5-BSA or NP_{23}-BSA in PBS overnight at 4°C, and then blocked with PBS containing 10% bovine serum at 4°C overnight. Splenocytes (5×10^5 cells/well) or BM cells (10^6 cells/well) were added to 96-well plates and incubated on the PVDF membrane at 37°C, 5% CO2 for 5 h. After incubation, PVDF membranes were washed with running ultra-pure water to lyse cells. They were then washed once with PBS containing 50 mM EDTA, followed by PBS containing 0·1% Tween-20 twice and PBS once again. Finally, membranes were double-stained with alkaline phosphatase (AP)-conjugated anti-mouse IgM and HRP-conjugated anti-mouse IgG1 antibodies (Southern Biotechnology). HRP and AP activities were visualized using 3-aminoethyl carbazole (Sigma, St. Louis, USA) and naphthol AS-MX phosphate/Fast Blue BB (Sigma) respectively. Colour development was stopped by thoroughly rinsing both sides of the PVDF membrane with demineralized water. The membranes were dried in the dark at RT. The spots were counted using a dissecting microscope (Motic# SMZ-161-BLED, Xiamen, China). All samples were run in 3–5 replicates.

Collagen-induced arthritis

To induce arthritis, 9- to 11-week-old, $FBW7^{f/f}$-$C\gamma1^{+/cre}$ and $C\gamma1^{+/cre}$ mice were injected intradermally at the base of the tail with 100 μg (in 100 μL) chick collagen type II (Chondrex, Redmond, WA, USA), which had been dissolved overnight at 4°C in 0·01 M acetic acid (Sigma) and emulsified in an equal volume of Complete Freund's Adjuvant (CFA, Chondrex). CFA was prepared by grinding 100 mg heat-killed *Mycobacterium tuberculosis* (H37Ra; Difco Laboratories) in 20 ml Incomplete Freund's Adjuvant (IFA, Chondrex). Three weeks after primary immunization, a booster immunization with 100 μg of chick collagen type II (CII) emulsified in IFA was given at the base of the tail [25, 26, 41]. Mice were observed for the onset of arthritis and evaluated for the duration of onset and severity of inflammation, with a score of 0–4 for each paw, and a combined clinical score was determined as described by Brand et al [25]. Thirty-six days after the booster immunization with CII, the mice were killed following retro-orbital bleeding. Mice were scored three times per week for 8 weeks. Serum levels of anti-mouse CII antibody (Chondrex) were determined by ELISA.

Measurement of collagen type II-specific antibodies

ELISA plates (Corning#9018, NY, USA) were coated with 10 μg/mL of chick type II collagen dissolved in Tris buffer (0·05 M Tris, containing 0·2 M NaCl, pH 7·4), and blocked with 2% bovine serum albumin for 2 h. Thereafter, sera from CIA mice were loaded onto these type II collagen-coated 96-well plates and incubated for 2 h at RT. Pooled sera from arthritic mice served as a positive control and reference standard. A standard curve was created for each assay by including serial dilutions of the reference sample on each plate. The reference sample was arbitrarily assigned an antibody concentration of 2 AU/ml. Serum levels of IgG1, IgG2a, IgG2b or IgG2c antibodies against type II collagen were measured by incubation with HRP-conjugated goat anti-mouse isotype-specific (IgG1, IgG2a, IgG2b or IgG2c; Southern Biotechnology) detection Abs, followed by TMB substrate. Optical density was measured at 450 nm. The antibody concentrations for each serum sample were obtained by reference to the standard curve.

Polymerase chain reaction (PCR) amplification and sequencing of Ig V186.2

Genomic DNA from sorted splenic GC B ($B220^+GL7^+Fas^+$) cells of NP–CGG immunized mice was extracted and frozen at −80°C until the PCR was carried out using the QIAamp DNA Micro Kit (Qiagen, Dusseldorf, Germany). PCR amplification and sequencing of variable heavy-chain region segments were carried out as previously described [42, 43]. Two sequential rounds of PCR were performed using high-fidelity PrimeSTAR DNA polymerase (Takara Bio, CA, USA). The two pairs of primers used are listed in Table S1. Primers corresponding to the V186.2 genomic DNA 5′ transcription start site and the intron JH2 sequence, respectively, were used for the first round of PCR (3 min 98°C preincubation; 25 cycles of 98°C 10 s, 55°C 5 s, 72°C 5 s; and 1 min at 72°C). 2 μl of this reaction mixture was reamplified for an additional 25 cycles (3 min 98°C preincubation; 25 cycles of 98°C 10 s, 51°C 5 s, 72°C 5 s; and 1 min at 72°C) using the second set of nested primers. The products were then visualized on 1·5% agarose gels, and a 300–400 bp band was detected and purified. After enzyme digestion and purification, the PCR products were cloned into the pcDNA3.1 vector. The recombinant plasmids were amplified by DH5α strain, extracted and sequenced. The chromatograms were identified by DNAStar software, and only high-quality sequences were considered Afterwards, sequences were blasted in the IgBlast database (https://www.ncbi.nlm.nih.gov/igblast/), which is linked to the ImMunoGeneTics V-QUEST online tool (IMGT).

Statistical analysis

Data on linear axes are depicted as mean ± standard deviation (S.D.) or mean ± standard error of the mean

(S.E.M). The statistical tests applied are stated in the legend of each figure. Statistical analysis was performed using GraphPad Prism software (GraphPad, San Diego, CA, USA). Generally, for comparisons of two groups, parametric data were analysed using two-tailed, a two-tailed, unpaired Student's *t*-test distribution with a confidence interval of 95%. Significant *p*-values are indicated in the figures by $*p < 0{\cdot}05$; $**p < 0{\cdot}01$; and $***p < 0{\cdot}001$.

RESULTS

FBW7 expression in various B-cell subsets

To investigate the potential intrinsic role of FBW7 in B cells, we characterized different B-cell subpopulations isolated from human tonsil and mouse spleens by FACS. The gating strategies for these cells are shown in Figure S1a,c. FBW7 expression in the different human B-cell subsets at the protein level is shown in Figure 1a and Figure S1b and at the RNA level in mice by real-time PCR in Figure 1b. Our results indicate that the level of FBW7 protein expression is significantly greater in human GC B cells relative to naïve B cells (Figure 1a,b). Western blotting further confirmed that FBW7 was expressed in both human centroblasts and centrocytes (Figure S1b). Consistent with these results, the mRNA expression pattern of FBW7 in mouse B-cell subsets established by searching the public database ImmGen (www.immgen.org) also indicates that FBW7 is expressed in most B-cell subsets and strongly expressed in GC B cells (Figure 1c,d). In addition, it may be seen that levels of FBW7 mRNA in B1 cells of the peritoneal cavity (Figure 1c) and plasma cells (Figure 1d) are higher than in other B-cell subsets.

The role of FBW 7 in B-cell homeostasis and the TI antibody response

FBW7 is expressed in B cells over the course of their development (Figure 1c,d). To investigate its role in B-cell development and function, we crossed FBW7 mice carrying the loxp flox alleles ($FBW7^{f/f}$) to CD19-Cre transgenic mice, in which the earliest deletion of loxP-flanked regions starts at the pro-B-cell stage and continues throughout B-cell development [44]. First, we analysed B-cell development in the bone marrow (BM), as defined by expression of B220, IgM or CD43. Although there were no significant changes in the overall percentage (Figure S2a) and the number (data not shown) of BM B cells, the percentages of the mature recirculating B cells and mature B cells were significantly reduced in $FBW7^{f/f}$-$CD19^{+/cre}$ mice relative to WT mice (Figure S2a). Correspondingly, peripheral $B220^{+}$B cells in spleens did not decrease markedly in $FBW7^{f/f}$-$CD19^{+/cre}$ mice (Figure S2b), but the number of B cells decreased sharply (Figure 2a). Likewise, $FBW7^{f/f}$-$CD19^{+/cre}$ mice had lower proportions of mature B cells in the spleen (Figure S2b). Staining splenic B cells for CD21 and CD23 revealed significantly fewer marginal zone (MZ) B and follicular (FO) B cells (Figure 2a). It was also found that the density of surface expression of CD23 (MFI) was lower in B cells (Figure S2c). Furthermore, the proportions and numbers of innate-like B1a and B1b cells were both reduced in the peritoneal cavity, suggesting that FBW7 might be necessary for the maintenance of B1 cells (Figure 2b). Similarly, the number of B2 cells in the peritoneum of $FBW7^{f/f}$-$CD19^{+/cre}$ mice was drastically reduced as well (Figure 2b). Consistent with this, $FBW7^{f/f}$-$CD19^{+/cre}$ mice showed a decreased percentage of B1 cells in spleens, especially B1b cells (Figure S2d).

The subsequent effects of FBW7 deficiency in B cells, which as shown above resulted in a reduction in the number and proportions of functional B cells, were reflected in their functional immune responses. To analyse the impact of FBW7 deficiency on antibody responses, we immunized $FBW7^{f/f}$-$CD19^{+/cre}$ and control mice with the T cell-independent antigen (Ag) NP-Ficoll, which induces immune responses dominated by $Ig\lambda^{+}$ NP-specific antibodies [45–49]. Both B1 and MZ B cells are considered to be major contributors to the TI-Ag antibody response. As expected, our results showed that the frequencies of IgM^{+} B cells and λ^{+} NP-specific B cells were both decreased in the spleens of $FBW7^{f/f}$-$CD19^{+/cre}$ mice 7 days after immunization (Figure 2c,d). NP-Ficoll elicits robust IgM and IgG3 antibody production in a T cell-independent fashion [50]. Strikingly, NP-Ficoll immunization of $FBW7^{f/f}$-$CD19^{+/cre}$ mice produced very low titres of IgG3 antibody compared to wild type, especially at day 14 after immunization (Figure 2e, right panel). We also observed lower IgM levels on day 7 after immunization but not thereafter (Figure 2e left panel). Taken together, these data show that humoral immune responses to the T-independent antigen NP-Ficoll were weakened in $FBW7^{f/f}$-$CD19^{+/cre}$ mice, particularly the IgG3 response.

BCR signalling is important for B-cell homeostasis by delivering survival signals to the cells. The decrease of peripheral mature B cells and peritoneal B1 cells in $FBW7^{f/f}$-$CD19^{+/cre}$ mice suggested that BCR signalling might be impaired. Thus, we purified splenic naïve B cells from $FBW7^{f/f}$-$CD19^{+/cre}$ and control mice and labelled them with the division tracking dye CFSE. They were then stimulated with anti-IgM or cultured without stimulation. The survival rate of unstimulated B cells lacking FBW7 and WT B cells was similar (Figure S3a,b). However, under stimulation with anti-IgM, the number (Figure S3c) and viability (Figure S3d) of FBW7-deficient B cells

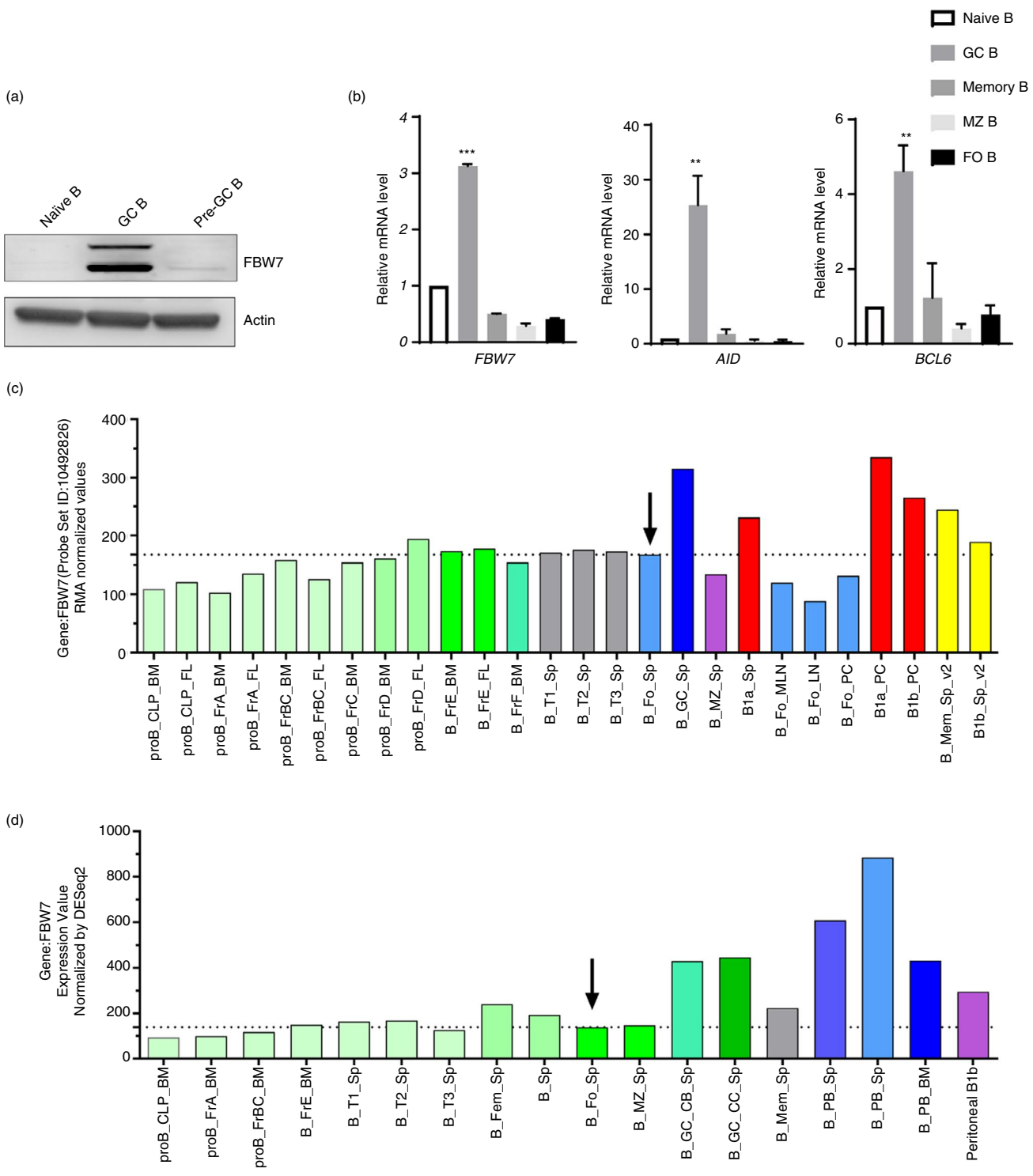

FIGURE 1 FBW7 expression in mouse and human B-cell subsets. (a). FBW7 expression in different B-cell subsets from human tonsil: Western blotting of FBW7 in sorted human B-cell subsets. Data are representative of two independent experiments. (b). FBW7 transcript levels in different B-cell stages of mice. Real-time RT-PCR analyses of FBW7 in naive/mature B, GC B, memory B, MZ B and FO B cells: Naïve, MZ and FO B cells were sorted from naïve mice. GC and memory B cells were sorted from mice immunized by NP-CGG. Experiments were performed twice in duplicate using cells pooled from several C57BL/6 mice. Expression was normalized to naïve B cells. Relative mRNA levels of BCL6 and AID were measured as the quality controls. Data in this figure are presented as mean ± SEM. All B cells were sorted by flow cytometry and detailed gating strategies are shown in Figure S1. (c,d). FBW7 transcript levels in mouse B-cell subsets from the indicated database (http://www.immgen.org/). (c). RNA-seq data (d). Microarray data. The dashed line represents the mRNA level of FBW7 in splenic FO B cells. GC, Germinal centre. CB, Centroblasts. CC, Centrocytes. MZ, marginal zone. FO, follicular. BCL6, B-cell lymphoma 6. AID, activation-induced cytidine deaminase. CLP, common lymphoid progenitor. PB, plasmablasts. PC, plasma cell

decreased significantly with increasing culture duration. In the unstimulated state, the size of FBW7-deficient and control B cells was similar, but after anti-IgM stimulation, the size of the surviving viable FBW7-deficient B cells was smaller than the control group (Figure S3e). This further indicates that the absence of FBW7 affected the activation and growth of cells stimulated by anti-IgM. Consistently, the proliferation of FBW7-deficient B cells was impaired on anti-IgM stimulation (Figure S3f).

Taken together, these results confirm that FBW7 contributes to the maintenance of B-cell homeostasis, particularly regarding numbers of normal mature B cells and B1 cells. In vivo, FBW7 deficiency in mature B cells and B1 cells results in an impaired T cell-independent antibody response. Moreover, the results show that FBW7 is important for BCR-mediated B-cell proliferation and survival.

The role of FBW7 in the GC reaction and TD primary antibody responses

To elucidate the role of FBW7 in regulating GC formation and function, conditional knockout FBW7$^{f/f}$-Cγ1$^{+/cre}$ mice were generated by crossing FBW7$^{f/f}$ mice with Cγ1-cre mice [51]. Expression of Cre recombinase is induced by germline Cγ1 transcription after T cell-dependent antigen immunization, resulting in the Cre-mediated deletion of loxP-flanked genes in the majority of GC B cells [51]. B-cell development in the BM, spleen and the serum Ig isotypes appeared to be normal in naïve FBW7$^{f/f}$-Cγ1$^{+/cre}$ mice (data not shown), in which any possible effects of FBW7 loss during early B-cell development could be circumvented. After immunization with the well-defined T cell-dependent Ag (4-hydroxy-3-nitrophenyl) acetyl (NP) conjugated with chicken γ-globulin (NP-CGG), the GC responses of FBW7$^{f/f}$-Cγ1$^{+/cre}$ and Cγ1$^{+/cre}$ mice were analysed on day 13 post-immunization. By flow cytometric analyses, we found that the proportion of splenic FBW7-null GC B cells and WT controls was similar (Figure 3a,b). Consistent with this, immunohistological analysis indicated no significant difference in the amount and size of GCs in spleens between FBW7$^{f/f}$-Cγ1$^{+/cre}$ and control mice (Figure S4a). T follicular helper (Tfh) cells provide an important signal for GC B survival and antibody production. Our results showed that the proportion of Tfh cells in GC was not significantly different in FBW7$^{f/f}$-Cγ1$^{+/cre}$ and WT mice (Figure S4b). To further investigate the impact of FBW7 deletion on GC B cells, centrocytes (CC) and centroblasts (CB) were distinguished by the expression of CXCR4 and CD86. We found that the ratio of CB to CC was increased by FBW7-deficiency (Figure 3c), suggesting that GC function may be compromised. Moreover, the levels of IgM$^-$GC B cells and IgG1$^+$GC B cells expressing class-switched BCRs were significantly reduced by FBW7 deficiency (Figure 3d,e and Figure S4c,d). These data indicate that Ig class-switching is impaired in FBW7-deficient GC B cells.

In vitro stimulation of naïve B cells with LPS plus IL-4 can be used to induce CSR. We found that 4 days after such stimulation, B cells derived from FBW7$^{f/f}$-CD19$^{+/cre}$ mice exhibited impaired CSR and significant reduction of IgG1$^+$IgM$^-$ class switched B cells relative to controls (Figure 3f and Figure S4e). However, FBW7-deficient B cells retained normal proliferative capacity and cell viability when stimulated by LPS plus IL-4, indicating that the CSR defect in FBW7$^{f/f}$-Cγ1$^{+/cre}$ B cells does not result from a defect in their proliferative capacity (Figure S4f,g).

Primary antibody responses after 13 days of NP-CGG immunization include the production of high-affinity and total (including high- and low-affinity) anti-NP IgG1 and anti-NP IgM. The levels of antibody and antibody-secreting cells (ASCs) were tested using two antigens with different ratios of NP/BSA (NP5-BSA and NP23-BSA). ELISA experiments were performed to measure titres of NP-binding antibodies in serum. Whereas NP-specific IgM titres were only marginally affected in the FBW7$^{f/f}$-Cγ1$^{+/cre}$ mice, the total (NP23-binding) and high-affinity (NP5-binding) NP-specific class-switched IgG1 antibodies were markedly impaired by FBW7-deficiency (Figure 4a). Likewise, FBW7-deficiency impaired the generation of class-switched total

FIGURE 2 FBW7 deficiency compromises T cell-independent immune responses. (a). Flow cytometric analysis of B-cell subsets in the spleen of unimmunized FBW7$^{f/f}$-CD19$^{+/cre}$ and CD19$^{+/cre}$ control mice. Splenocytes were stained with B220, CD21 and CD23 antibodies to distinguish FO B (B220$^+$CD21$^+$CD23^{hi}) and MZ B (B220$^+$CD21^{hi}CD23^{lo}) cell subsets. (b). Flow cytometric analysis of peritoneal B-cell subsets. Peritoneal B-2 cells (B220^{hi}CD5$^-$), B-1a B cells (B220^{low}CD5$^+$) and B-1b B cells (B220^{low}CD5$^-$) were identified. FBW7$^{f/f}$-CD19$^{+/cre}$ and CD19$^{+/cre}$ control mice were immunized with 50 μg NP-Ficoll (dissolved in PBS). Sera were collected on the indicated days (c–e). (c). Flow cytometric analysis of the expression of IgM on the surface of B220$^+$ B cells (MFI) and the proportion of IgM$^+$ B cells in spleens on day 7. (d). Flow cytometric analysis of NP-specific lambda$^+$ B cells in spleens of mice on day 7 after immunization. All representative dot plots are shown on the left and individual values for each mouse are shown on the right (a–d). (e). NP-specific IgM, IgG3 antibodies (NP23-binding) in the sera were measured by ELISA on the indicated days using 4–8 mice per group. *p* values were determined using the unpaired two-tailed Student's *t* test (a–d) or two-way analysis of variance (ANOVA) with multiple comparisons testing (e). Data were combined from two independent experiments (a,b,e) or are representative of two independent experiments (c,d). Error bars show means ± SEM (a–e). *$p < 0{\cdot}05$; **$p < 0{\cdot}01$; ***$p < 0{\cdot}001$; ****$p < 0{\cdot}0001$. FACS, flow cytometry; MFI, mean fluorescence intensity

Immunology
The Journal of cells, molecules, systems and technologies
British Society for immunology

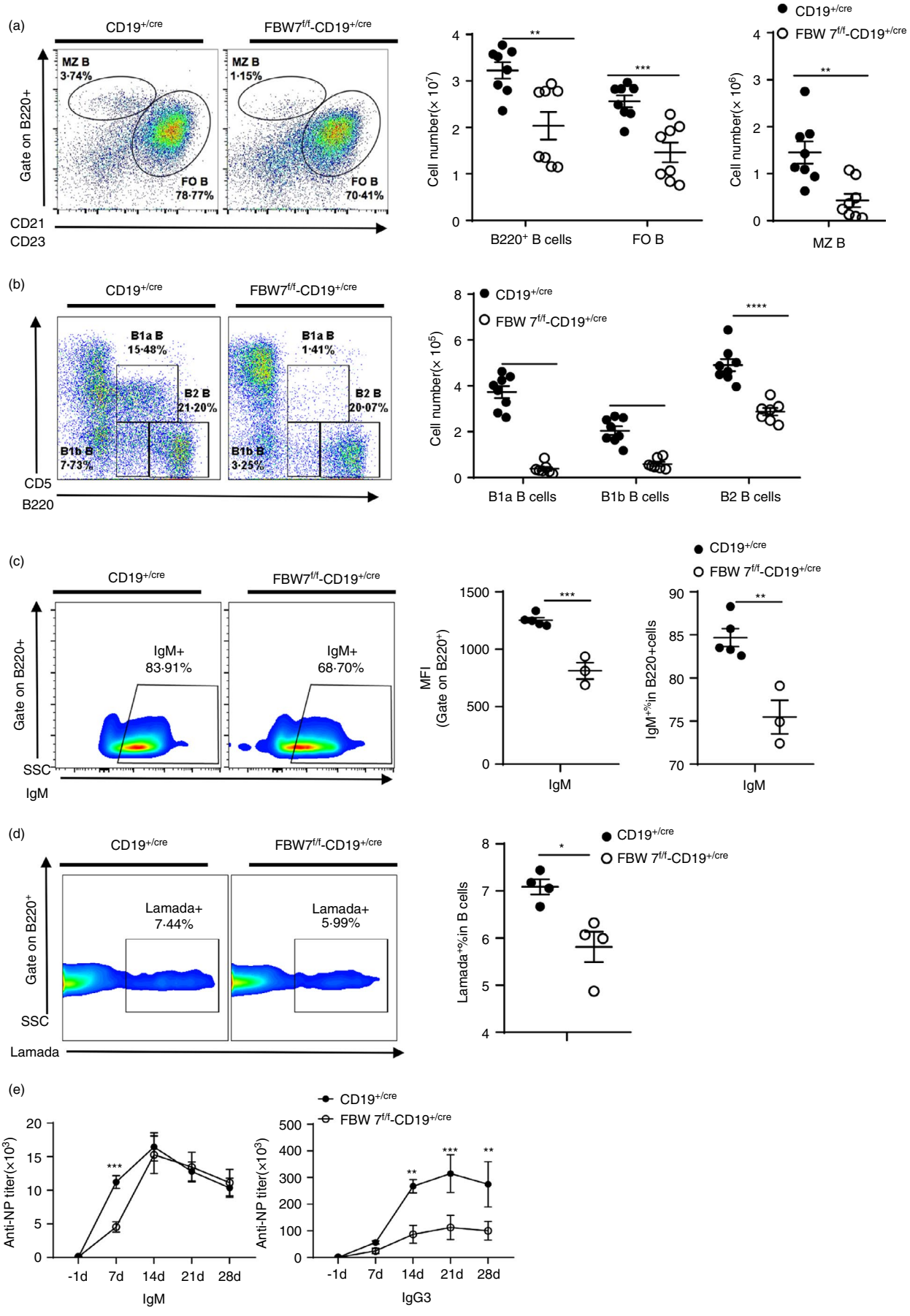

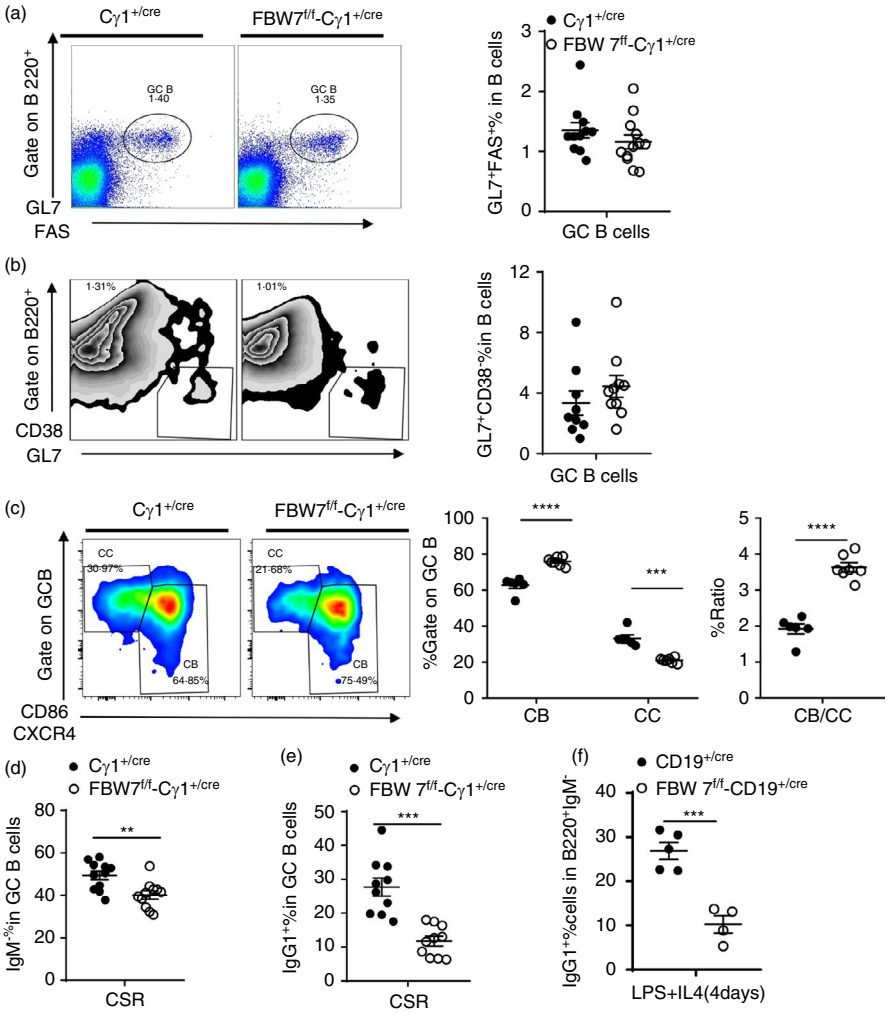

FIGURE 3 FBW7 deficiency does not affect GC formation but affect class switching. FBW7$^{f/f}$-Cγ1$^{+/Cre}$ and Cγ1$^{+/Cre}$ control mice were immunized with NP-CGG in alum 13 days prior to analysis of splenocytes (a–e). Flow cytometric analysis of (a). B220^{+}Fas^{+}GL7^{+} GC B cells (b). B220^{+}CD38^{-}GL7^{+} GC B cells in spleens. (c). GC B cells (B220^{+}GL7^{+}FAS^{+}) were further distinguished as CB (CXCR4^{high}CD86^{low}) and CC (CXCR4^{low}CD86^{high}). Flow cytometric analysis of (d). IgG1^{+}class-switched GC B cells (B220^{+}GL7^{+}FAS^{+}) and (e) IgM^{-}class-switched GC B cells (B220^{+}GL7^{+}FAS^{+}). (f). Flow cytometric analysis of induced class-switched B cells (IgG1^{+}IgM^{-}B220^{+}). Purified naïve B cells from FBW7$^{f/f}$-CD19$^{+/cre}$ and CD19$^{+/cre}$ control mice were labelled with CFSE and stimulated to induce class switching using LPS (20 μg/ml) and IL-4 (50 ng/ml) for 4 days. Individual values from each mouse are shown. In all statistical graphs, dots represent individual mice (a–f). Representative dot plots of FACS are shown in the left panel of 3a–c or Figure S4c–e. Error bars are means ± SEM, and *p* values are determined by unpaired two-tailed Student's *t* test. **p* < 0·05; ***p* < 0·01; ****p* < 0·001; *****p* < 0·0001. GC, germinal centre; CB, centroblasts; CC, centrocytes; FACS, flow cytometry

and high-affinity NP-specific ASCs (Figure 4b). In addition, we found that the ratio of NP5/NP23 IgG1 titres in FBW7$^{f/f}$-Cγ1$^{+/cre}$ mice was significantly reduced compared to the control group, indicating impaired affinity maturation of antibody in these mice (Figure 4c). These data document that FBW7$^{f/f}$-Cγ1$^{+/cre}$ mice exhibit an impaired antibody response, particularly in their ability to produce high affinity (NP5-binding) class-switched (IgG1) antibodies (Figure 4a–c). Taken together, these results demonstrate that FBW 7 ablation in B cells at the GC stage has no significant impact on GC formation, but does affect two critical GC functions, namely CSR and antibody affinity maturation, which were severely impaired.

Another major characteristic of GC B cells is the somatic hypermutation (SHM) of Ig genes, which provides the substrate for affinity-driven clonal selection, leading to affinity maturation of antibodies. On day 13 after immunization with NP-CGG, the typical gene fragment V_H186·2 encoding high-affinity NP-specific antibodies dominates the BCR repertoire [52, 53]. To determine the role of FBW7 in regulating Ig gene SHM, the BCR mutation frequency in NP-CGG–immunized FBW7$^{f/f}$-Cγ1$^{+/cre}$ and control mice were examined by genomic DNA sequencing. GC B cells were sorted for sequencing of VDJ segments of the V_HJ558 family of Ig H-chain genes. Our results showed that there was no significant clonal type

Immunology
The Journal of cells, molecules, systems and technologies
British Society for immunology

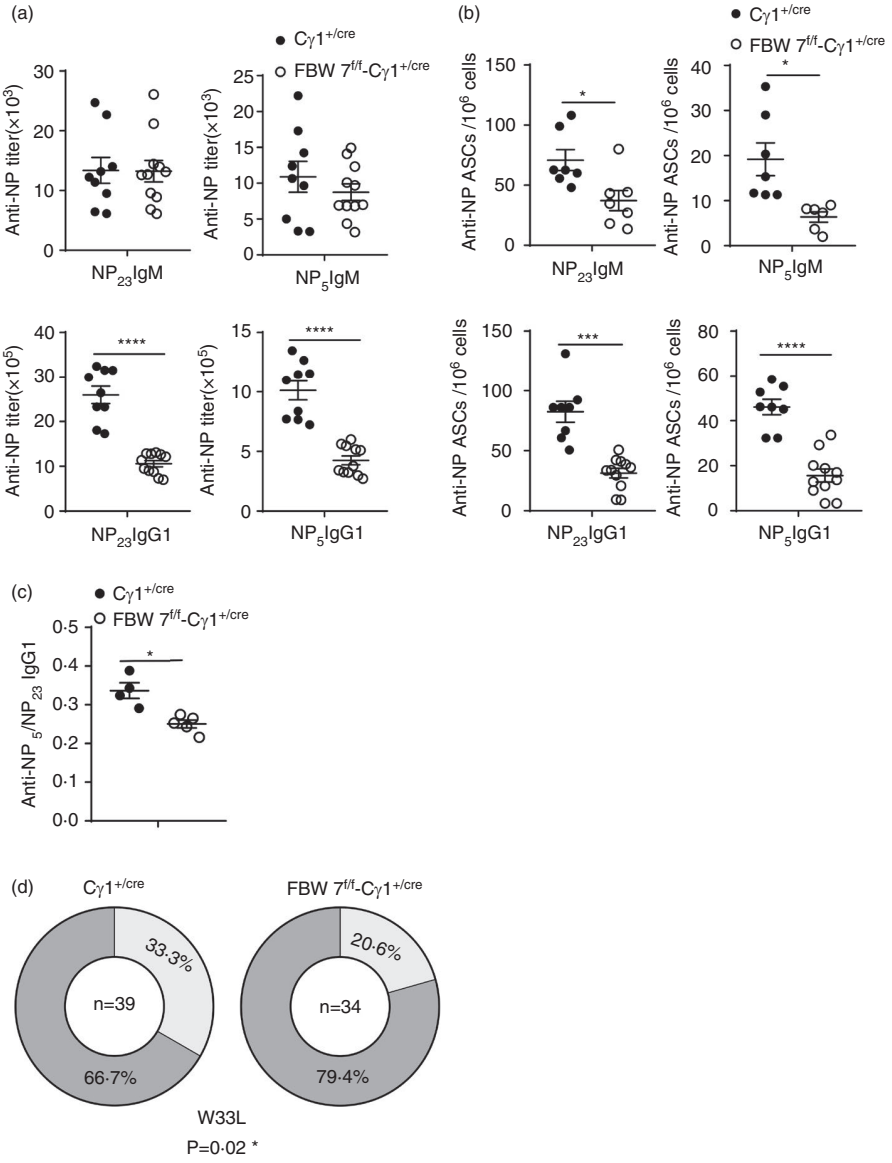

FIGURE 4 FBW7 deficiency impairs antibody affinity maturation. FBW7$^{f/f}$-Cγ1$^{+/Cre}$ and Cγ1$^{+/Cre}$ control mice were immunized with NP-CGG for 13 days. Sera were collected before immunized mice were killed. (a). Concentrations of NP-specific IgM (upper panel) and IgG1 (lower panel) in the serum were determined by ELISA. NP-23 indicates total Ig and NP-5 suggests high-affinity Ig. (b). NP-specific IgM (upper panel) and IgG1 (lower panel) ASCs in the spleen were evaluated by ELISPOT. Data were pooled from three experiments (a,b). (c). NP_5/NP_{23} antibody titre ratio in immunized mice. Data are representative of three experiments. In all statistical graphs, dots represent individual mice. Error bars show means ± SEM, and *p* values were determined by an unpaired two-tailed Student's *t* test (a–c). (d). The frequency of W33L mutations in the VH186.2 heavy chain as determined by sequencing. The total numbers of clones sequenced are indicated at the centre of the pie charts. Statistical analysis was done with the chi-square test. *$p < 0{\cdot}05$; **$p < 0{\cdot}01$; ***$p < 0{\cdot}001$; ****$p < 0{\cdot}0001$. Ig, immunoglobulin. ASCs, antibody-secreting cells. ELISA, enzyme-linked immunosorbent assay. ELISPOT, enzyme-linked immuno-spot assay

shift of IgH-chain genes between wild-type GC B cells and FBW7-null GC B cells (Figure 5a). Ig mutation rates in VH186.2 clones and analogous clones exhibited no significant differences in GC B cells from FBW7 conditional knockout or WT mice (Table 1 and Figure 5b,c). Therefore, our data demonstrate that the SHM machinery is normal in FBW7$^{f/f}$-Cγ1$^{+/cre}$ mice. Notably, in line with the reduced high-affinity NP-specific antibody titre and numbers of ASCs in immunized FBW7$^{f/f}$-Cγ1$^{+/cre}$ mice (Figure 4a–c), we found a greatly reduced fraction of FBW7-deficient GC B-cell clones carrying the W33L mutation (Figure 4d). It has been reported that clones carrying this mutation can produce antibodies with an approximately 10-fold increased affinity for the NP antigen [54]. Taken together, all these results indicate that FBW7 is critical for affinity-based selection.

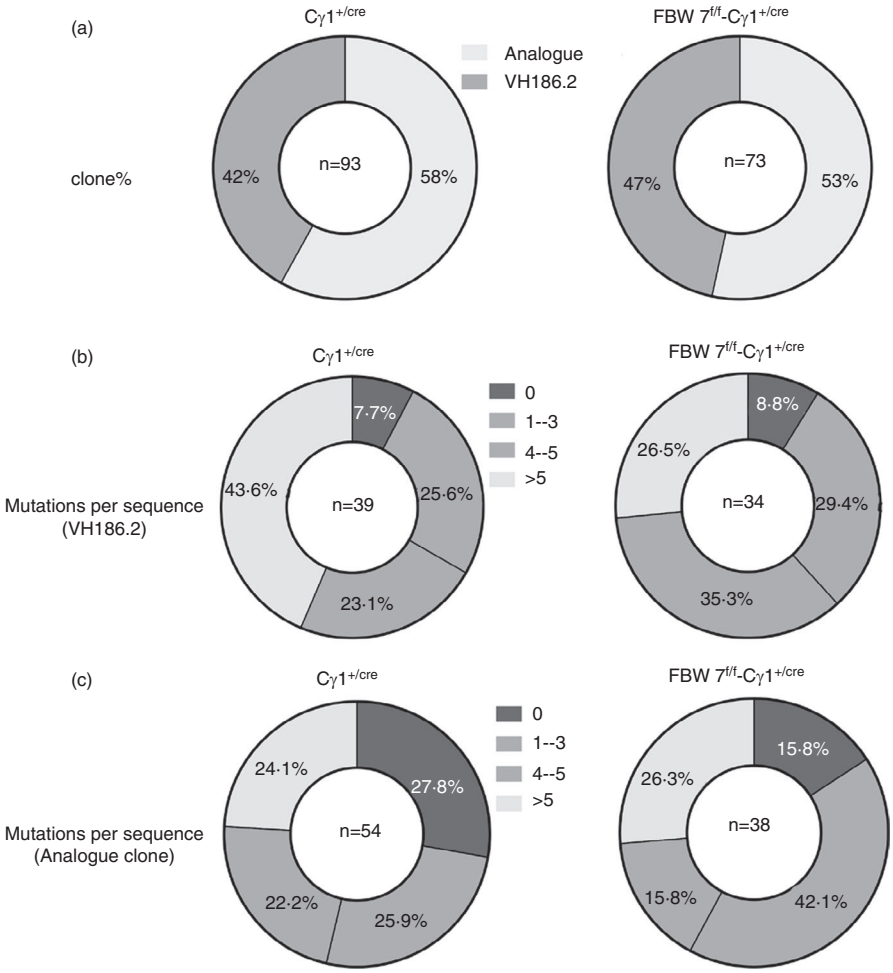

FIGURE 5 Normal somatic hypermutation in FBW7-null GC B cells. On day 13 following immunization with NP-CGG, V_H segments from sorted GC B cells ($B220^+GL7^+FAS^+$) of two $FBW7^{f/f}$-$C\gamma1^{+/Cre}$ mice and three $C\gamma1^{+/Cre}$ control mice were sequenced and analysed. (a). Percentage of sequences containing VH186.2 and analogue genes. (b). Percentages of sequences containing 1–3, 4–5 or >5 point mutations in VH186.2 clones. (c). Percentages of sequences containing 1–3, 4–5 or >5 point mutations in analogous clones. Numbers in the centre of the pie charts indicate the numbers of clones sequenced. Statistical analysis was done with chi-square test

Cγ1 cre-mediated FBW7 gene deletions are mainly present in the GC B cells that usually account for 2–10% of total B cells. To further investigate the underlying molecular mechanisms responsible for the defective GC function in conditional FBW7-deficient mice, including CSR and affinity maturation, we performed a mechanistic study using B cells derived from $FBW7^{f/f}$-$CD19^{cre+}$ mice, in which all the B cells lack FBW7 expression. To this end, naive B cells were stimulated by LPS plus IL-4 in vitro for 4 days. We then measured activation-induced cytidine deaminase (AID) protein levels and found that they were similar in both FBW7-deficient B cells and controls. This suggests that the defective CSR in FBW7-deficient GC B cells was not the result of AID alteration (Figure S5a). The normal expression of AID, a key factor for both CSR and SHM, further explains why the SHM of BCRs can take place normally in FBW7-null GC B cells. Likewise, there were no significant differences between B cells from FBW7f/f-$C\gamma1^{+/cre}$ mice and controls in terms of other transcription factors essential for GC B-cell function, including interferon regulatory factor 4 (IRF4), Forkhead box O1 (FOXO1) and paired box 5 (PAX5) (Figure S5a). The transcriptional repressor B-cell lymphoma 6 protein (BCL6) is essential for the initiation and maintenance of the GC reaction. Mice lacking BCL6 cannot form GCs nor produce high-affinity antibodies. Multiple signalling pathways contribute to BCL6 downregulation. For these reasons, we also measured BCL6 expression at an earlier time-point and found that its expression was indeed down-regulated in FBW7-null B cells (Figure S5b).

Collectively, we conclude that deletion of FBW7 in GC B cells severely impairs GC function, leading to suppressed CSR and diminished antibody affinity maturation in primary antibody responses.

The role of FBW7 in a secondary antibody response

Another critical function of the GC reaction is the generation of memory B cells and long-lived antibody-secreting cells. To further study the role of FBW7 in the functional maturation of GC reaction, the memory response to secondary immunization with NP-CGG was evaluated. Following secondary immunization, sera from $FBW7^{f/f}$-$C\gamma1^{+/cre}$ mice and control mice were collected at different times and NP-specific antibodies were measured by ELISA. We found that the titres of NP-specific class-switched (IgG1) antibodies were lower in

Immunology
The Journal of cells, molecules, systems and technologies
British Society for immunology

TABLE 1 Mutation analysis of VH gene segment in GC B cells

	$C\gamma1^{+/cre}$	FBW $7^{f/f}$-$C\gamma1^{+/cre}$
VH186.2 clones		
Mutation rate (%)		
Total	1·76	1·48
CDRs (1–2)	3·85	3·25
FRs (1–3)	1·35	1·13
R/S ratio		
CDRs (1–2)	8·75 (70/8)	16·67 (50/3)
FRs (1–3)	3·00 (90/30)	3·00 (69/23)
Analogue clones		
Mutation rate (%)		
Total	1·25	1·41
CDRs	2·2	2·1
FRs	1·06	1·28
R/S ratio		
CDRs	3·75 (45/12)	8·50 (34/4)
FRs	2·54 (99/39)	1·61 (71/44)

Note: Percentage of base pairs that are mutated.

Abbreviations: CDRs, complementarity-determining regions; FRs, framework regions; R, replacement; S, silent.

$FBW7^{f/f}$-$C\gamma1^{+/cre}$ mice than controls (Figure 6a). The deficiency in the secondary antibody response was particularly profound when NP-specific class-switched (IgG1) ASCs were measured in the spleen and bone marrow. Consistent with the data on NP-specific antibodies, the numbers of ASCs were significantly reduced in $FBW7^{f/f}$-$C\gamma1^{+/cre}$ mice, particularly the high-affinity (NP5-binding) ASCs (Figure 6b,c). In addition, the proportion of memory B cells with the $B220^{+}CD138^{-}CD38^{+}IgG1^{+}$ phenotype in the BM was significantly lower in $FBW7^{f/f}$-$C\gamma1^{+/cre}$ mice than WT control mice 4 weeks after primary immunization (Figure 6d). The frequency of this cell population in the spleen was also lower than in the control mice, although not to a significant extent. Thus, the deletion of FBW7 in GC B cells impairs GC functional maturation, leading to a diminished memory antibody response, and decreased long-lived ASCs.

FBW7 deficiency in GC B cells ameliorates the development and pathogenesis of CIA

To explore whether FBW7 is essential for the production of pathological antibodies that are indispensable for the pathogenesis of an autoimmune disorder, we employed the model of collagen-induced arthritis (CIA) in $FBW7^{f/f}$-$C\gamma1^{+/cre}$ mice. Our data show that FBW7-deficient mice exhibited a slower disease induction phase than the WT controls. Disease onset was delayed and disease severity significantly reduced in the FBW7-deficient mice (Figure 7a). In addition, disease incidence was also markedly lower in the $FBW7^{f/f}$-$C\gamma1^{+/cre}$ mice (Figure 7b). Joint destruction was significantly milder in FBW7 conditional knockout mice according to X-ray analysis of the inflamed paws during the onset of CIA (day 10 after the booster immunization with collagen) (Figure 7c). Consistent with this, levels of anti-CII autoantibodies in the sera of $FBW7^{f/f}$-$C\gamma1^{+/cre}$ mice were lower than WT controls, especially the IgG1 and IgG2a isotypes (Figure 7d). Thus, defects in antibody production in $FBW7^{f/f}$-$C\gamma1^{+/cre}$ mice ameliorate CIA, suggesting that FBW7 acts as a positive regulator of B-cell function in the CIA model.

DISCUSSION

In the present study, we analysed the expression profiles and function of FBW7 in human and mouse B-cell subsets. We found that FBW7 was highly expressed in B1 cells and GC B cells, although it was also found in other B-cell subsets. Using two conditional gene knockout mouse models, we determined that FBW7 plays critical roles in B-cell responses and in the pathogenesis of autoimmune arthritis in the mouse CIA model.

First, regarding B-cell development, we found that FBW7 was dispensable at the early stages in the BM, but it was necessary for the survival of mature recirculating B cells. These cells in the periphery are considered to be long-lived cells secreting Abs against blood-borne pathogens [55]. Next, we found that FBW7 deficiency led to a sharp decline in the numbers and percentages of peripheral mature B cells and peritoneal B1 cells. The reduction of B1 cells in the peritoneal cavity and peripheral mature B cells are common features of mice with impaired BCR signalling [56, 57]. B1 cell development is self-renewing and cannot be replenished continuously; its development depends on stronger BCR signalling than required for maintaining FO and MZ B cells [57, 58]. These findings implied that FBW7 might positively regulate BCR signalling during B-cell development and maturation. Indeed, we found that FBW7-null B cells exhibited reduced cell survival and proliferation after BCR cross-linking in vitro, consistent with previous reports [39]. These results further emphasize the role of FBW7 as a pro-survival factor in the context of normal or cancerous B cells.

MZ and B1 cells are the chief contributors to TI-2 antigen responses by producing IgM and IgG3 antibodies. In the extrafollicular response to low doses of NP-Ficoll, IgG3 isotype antibody can be produced without induction of germinal centres [47] and SHM [59]. CSR can take place outside the GCs, following B-cell activation [60]. In

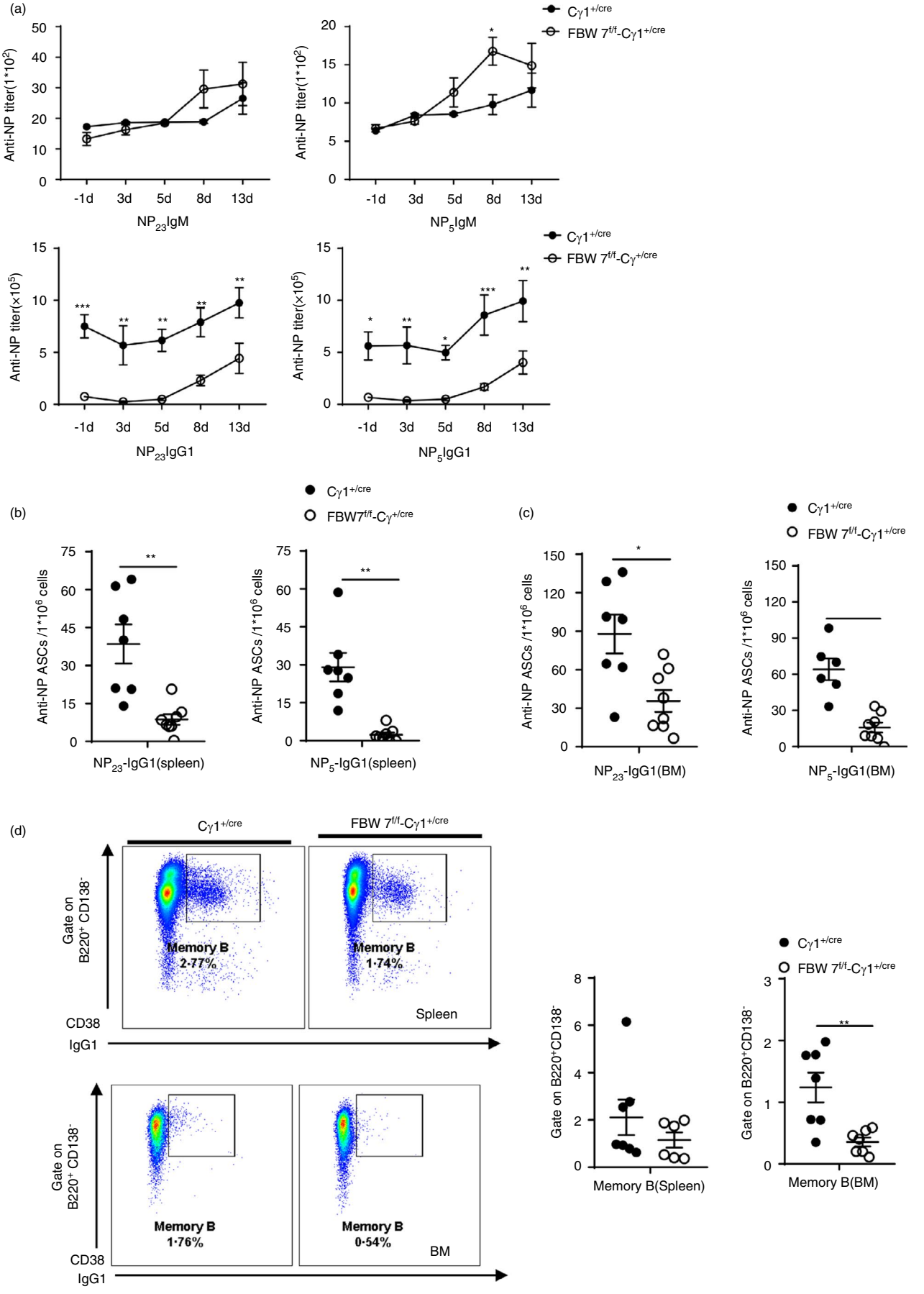
(a)
Cγ1+/cre
FBW 7f/f-Cγ1+/cre
Anti-NP titer(1*10²)
NP23IgM
NP5IgM
Anti-NP titer(×10⁵)
NP23IgG1
NP5IgG1
-1d
3d
5d
8d
13d
(b)
FBW7f/f-Cγ+/cre
Anti-NP ASCs /1*10⁶ cells
NP23-IgG1(spleen)
NP5-IgG1(spleen)
(c)
NP23-IgG1(BM)
NP5-IgG1(BM)
(d)
Gate on B220+ CD138-
CD38
IgG1
Memory B 2·77%
Memory B 1·74%
Spleen
Memory B 1·76%
Memory B 0·54%
BM
Memory B(Spleen)
Memory B(BM)

FIGURE 6 FBW7 is required to mount a recall immune response. An NP-specific memory B-cell response was recalled by i.p. injection of 20 μg NP-CGG in PBS 2 month after the first immunization (a–c). (a). Concentrations of NP-specific IgM (upper panel) and IgG1 (lower panel) in the sera were determined by ELISA. The sera were isolated 1 day before and 3, 5, 8 and 12 days post-secondary immunization. NP-23 indicates total Ig and NP-5 suggests high-affinity Ig. *p* values were analysed using a two-way analysis of variance (ANOVA) with multiple comparisons test. $N = 5$ in the FBW7$^{f/f}$-Cγ1$^{+/Cre}$ group and $N = 4$ in the Cγ1$^{+/Cre}$ control group. NP-specific long-lived IgG1 ASCs in the (b) spleen and (c) bone marrow were evaluated by ELISPOT. (d). Percentages of memory B cells in spleen were evaluated by flow cytometry on 28 days after NP-CGG immunization. Each symbol represents one mouse, and *p* values are determined by unpaired two-tailed Student's *t* test (b–d). Error bars show means ± SEM, and data are representative of three independent experiments (a–d). *$p < 0{\cdot}05$; **$p < 0{\cdot}01$; ***$p < 0{\cdot}001$; ****$p < 0{\cdot}0001$. Ig, immunoglobulin. ASCs, antibody-secreting cells

the case of NP-Ficoll, MZ B cells are consider to be the predominant responders [9]. After immunization with NP-Ficoll, we found that NP-specific IgG3 antibodies in FBW7-deficient mice were at almost the same low levels as controls at day 7 but were markedly lower than in controls at all later time-points tested. This clearly shows the importance of FBW7 for the development of full IgG3 responses. In contrast, the NP-specific IgM titre was not affected at later time-points, but was somewhat reduced at day 7. These results may suggest that FBW7 could be involved in other processes additional to maintaining peritoneal B1 cell and peripheral mature B-cell homeostasis, which impact IgM responses early on but are compensated for by other mechanisms later in the response. FBW7-deficient B cells showed less degraded IκBα and low p65 levels after BCR stimulation, suggesting lower canonical NF-κB signalling [39]. The NF-κB complex formed in BCR-activated B cells is primarily composed of the subunits p50, p65 and c-Rel. B cells lacking p65 proliferate well but have a defect in switching to IgG3, which was associated with a decrease in γ3 germline CH gene expression [61]. Therefore, FBW7 contributes to TI-2-dependent IgG3 antibody production. These results might also imply a role for FBW7 in the antibody CSR.

At the germinal centre stage, we found that FBW7 deletion did not affect the proportion of GC B cells and GC formation, in line with a previous report [39]. However, it did affect the proportions of centroblasts and centrocytes, respectively. Mature GC is divided into two functionally and physically distinct regions: the dark zone (DZ), where cell expansion and Ig SHM occurs, and the light zone (LZ), where B cells undergo CSR and are selected based on the affinity of their BCRs. FBW7 was shown to be expressed in CC and CB. The increased CB/CC ratio documented here suggested that loss of FBW7 at the germinal centre stage might influence the class switching and antibody affinity selection of GC B cells.

Our results showed that class-switched GC B cells, ASCs and antibody were all decreased in mice with FBW7 genetic ablation. Isotype-switched B cells can only appear after normal cell division, suggesting that the observed reductions of IgG1$^+$ or IgM$^-$class switched GC B cells might be due to defective proliferation of the FBW7-null B cell in response to BCR signalling [62]. However, our results showed that cell viability and proliferation were normal in FBW7-deficient B cells, when the CSR was induced by LPS plus IL4 stimulation in vitro. In addition, it has been reported that activation of BAFF signalling, CD40 signalling, or IL-4 signalling could rescue the survival defect of FBW7-null B cells after activation via BCR signalling [39]. B cells can be exposed to multiple stimuli in the GC stage. Therefore, the impaired CSR was not the result of a proliferation defect. The dynamics of germinal centre B cells are much more complex and involve a multitude of pathways and selection mechanisms. GC B cells undergo clonal expansion and SHM in the DZ and their clonal expansion provides a large template library for SHM, which is crucial for the diversification of the BCR repertoire. We found that the percentage of centroblasts in GC B cells was not decreased in the absence of FBW7. In addition, the absence of FBW7 in GC B cells did not affect normal mutations in Ig gene composition in the responding B-cell repertoire, which also indicates that the proliferation of GC B was not affected by FBW7 deficiency in the germinal centre reaction in vivo. Therefore, the exact function of FBW7 in vivo may depend on the type of antigenic stimulation and the microenvironment of the secondary lymphoid structures in which immune processes take place.

Importantly, in response to T-dependent antigens, the formation of early memory B cells was normal upon loss of FBW7 (data not show), while the frequency of long-lived class-switched memory B cells (IgG1$^+$ CD38$^+$ CD138$^-$B220$^+$) was markedly reduced in BM and spleen. This may be a consequence of the deficit in CSR. All the above results indicate that FBW7 plays an important role in the CSR process.

Both SHM and CSR require AID, which is expressed mainly in activated B cells of the germinal centre [63]. Mice and humans deficient in AID form large T cell-dependent germinal centres but have minimal hypermutation and Ig class switching [64]. We found that CSR after FBW7 deletion was impaired, but SHM was normal, which is consistent with the unaltered expression of AID in vitro and suggests that AID is not involved in the FBW7-mediated regulation of germinal centre function. Additionally, a lower percentage of GC B cells with the W33L substitution, a well-established readout of high-affinity antibody

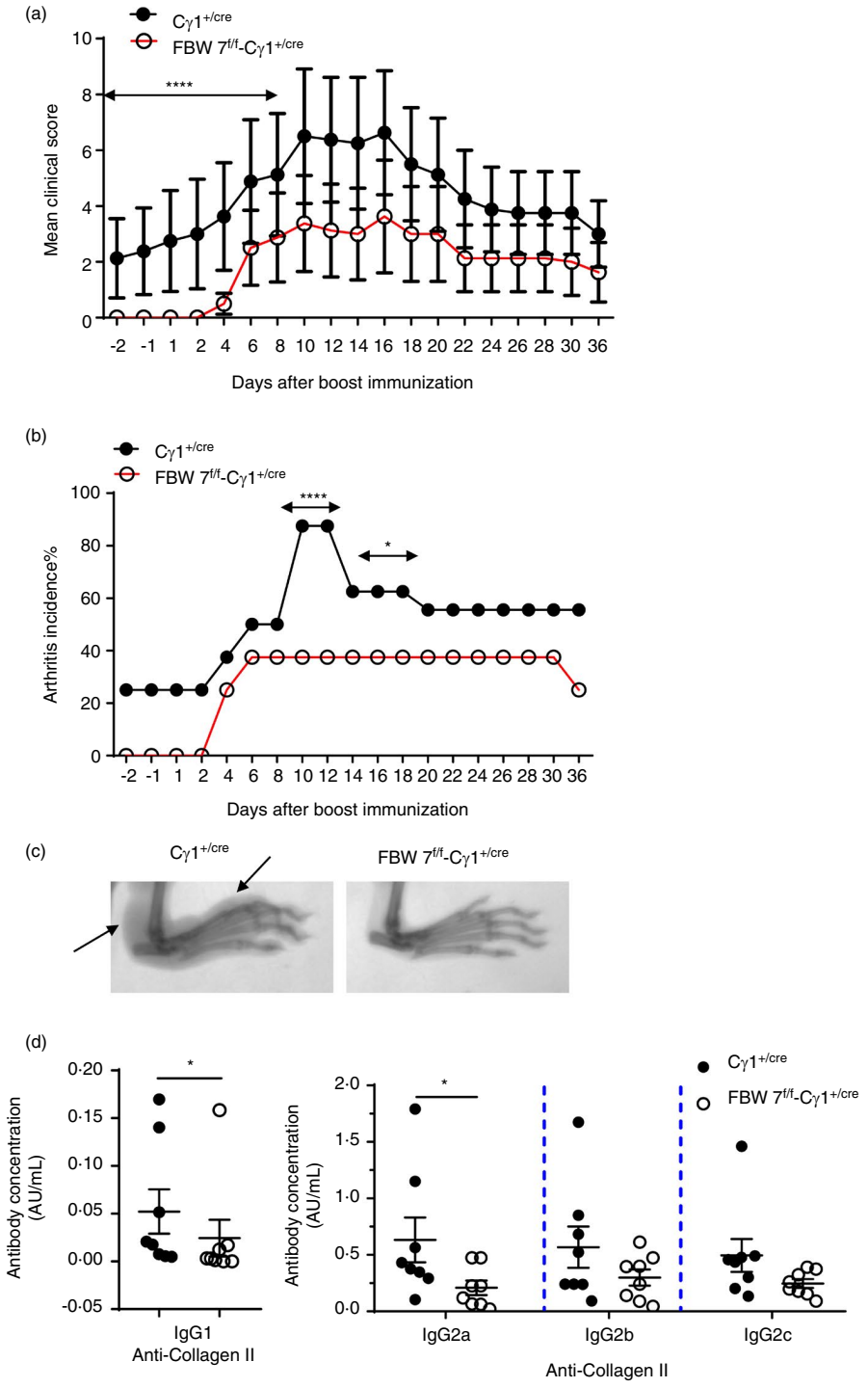

FIGURE 7 FBW7 deficiency in GC B cells attenuates CIA. FBW7$^{f/f}$-Cγ1$^{+/Cre}$ and Cγ1$^{+/Cre}$ control mice were i.d. immunized with chicken collagen II followed by a booster injection after 3 weeks. (a) Mean clinical score and (b) incidence of arthritis. FBW7$^{f/f}$-Cγ1$^{+/Cre}$ (open circles) and Cγ1$^{+/Cre}$ (closed circles) mice were evaluated until the end of experiment (day 36 after boost immunization). (c) X-ray analysis of the diseased paws of mice 10 days after immunization. Arrows indicate soft tissue swelling. (d) CII-specific IgG1 antibody levels in the serum were determined by ELISA 36 days after boost immunization. *p* values are determined by the Mann–Whitney nonparametric (two-tailed) test (a, d) or Chi-Square test (b). Values are expressed as mean ± SEM (a, d). Data are representative of two independent experiments with 8 mice in each group. *$p < 0{\cdot}05$; **$p < 0{\cdot}01$; ***$p < 0{\cdot}001$; ****$p < 0{\cdot}0001$. CIA, collagen-induced arthritis; CII, collagen type II. ELISA, enzyme-linked immunosorbent assay

for the NP response, suggested a defect in affinity maturation of FBW7-deficient GC B cells, which in turn could reflect inefficient cell selection.

During the germinal centre stage, many key regulators are involved in the initiation, development and differentiation of GC. FOXO1 is highly expressed in human and mouse GC B cells and is restricted to DZ B cells [65]. FOXO1 deletion impairs affinity maturation and IgG1 class switch recombination, but the SHM frequency is similar in WT and Foxo1-null GC B cells [65–67]. IRF4 plays an important role in the early initiation phase of GC formation and antibody class switching [68–70]. PAX5 binds to the promoter region of *Aicda* and activates its expression. Alternatively, PAX5, E2A and AID interact directly to form a complex which contributes to directing AID to the Igh locus for effecting CSR [71]. The transcription factor BCL6 is critical for germinal centre formation, and BCL6-deficient mice completely lacked GC_S and affinity maturation [72]. In our limited results, only a decrease in BCL6 expression was observed. Under the conditions of in vitro

induction of CSR employed here, the reduced expression of BCL6 may be one of the reasons for the impaired GC function caused by FBW7 deficiency.

FBW7 functions as the substrate recognition component of an SCF-type E3 ubiquitin ligase. It controls the proteasome-mediated degradation of various substrates in different cells and physiological environments. Phosphorylation of the Cdc4 phosphodegron (CPD) region is a prerequisite for the degradation of these substrates. Of the reported substrates that can be degraded by FBW7 [30, 73], most participate in germinal centre reactions as positive regulators [74], such as c-Myc [75, 76], MCL-1 [77] and STAT3 [78, 79]. We found that after FBW7 deletion, although GC formation was not affected, function was impaired, indicating that excessive substrate accumulation could also disturb the balance and impair GC function. c-Myc is required in both early and late initiation of GC formation, but is not expressed by proliferating centroblasts, where it is repressed by BCL6. In addition, c-Myc is required for GC maintenance in the later GC reaction. With the help of Tfh cells, c-Myc is transiently induced and upregulated in a small fraction of centrocytes with high-affinity BCRs. The selected c-Myc$^+$ GC B cells then migrate to the DZ for the next round of proliferation and SHM [74]. It has been reported that residual phosphorylation of Thr58 and Ser62 within the c-Myc CPD domain is an essential step for FBXW7-mediated degradation. Phosphorylation of Thr58 in c-Myc is mediated by GSK3β and is dependent on the prior phosphorylation of Ser-62 mediated by the Ras-Raf-MEK-ERK kinase cascade and/or CDKs [80]. During the germinal centre response, multiple signalling pathways are involved, such as BCR signalling, CD40 signalling and cytokines (IL-4, IL-21). In vitro CSR induction experiments can only partially simulate GC function. The dynamics of GC B cells greatly increases the difficulty of mechanistic research. We hypothesized that FBW7 degrades different substrates in different GC B subsets by activating different kinases (GSK3β, CDKs, etc.) to mediate the phosphorylation of CPD domains under specific signals. It has been reported that the major kinase GSK3β, which mediates phosphorylation of FBW7 substrates, converts to an inactive form on CD40 and IL-21 signalling [81]. Therefore, we hypothesized that FBW7 might mediate the degradation of c-Myc through GSKβ in DZ. However, other unknown substrates independent of GSK3 may also be present in LZ. Thus, the phenotypes we found might be the result of changes in multiple substrates. Accumulation of FBW7 substrates in response to ablation of FBW7 occurs in a cell-specific manner, leading to differences in the phenotypic consequences of FBW7 deletion. The molecular mechanism of FBW7-mediated B-cell responses in germinal centre reactions needs elucidation and will be the focus of our work in future. Gene expression profiling (GEP) of isolated FBW7-deficient GC B cells or GC B-cell subsets (centroblasts and centrocytes) may provide valuable information in this respect.

The production of class-switched high-affinity autoantibodies derived from organized GCs is a hallmark of many autoimmune inflammatory diseases, including rheumatoid arthritis (RA) [82, 83]. Most RA patients have circulating class-switched autoantibodies (e.g. ACPAs), and this is a well-documented risk factor for greater disease severity [84]. Therapeutic B-cell depletion using anti-CD20 antibody (rituximab) underscores the importance of B cells in maintaining disease activity in RA [85]. However, B-cell depletion therapy increases the risk of infection and many challenges remain in the treatment of RA. Treatment regimens should be developed to suppress humoral autoimmunity while balancing the immune response capacity. Therefore, targeting the GC reaction could allow for therapeutic interventions that are more specific than general B-cell depletion. Thus, we hypothesized that by targeting key regulatory factors of the GC response, the production of pathogenic autoantibodies could be limited, and thus, the inflammatory response could be inhibited. Based on the effect of FBW7 deletion on B-cell antibody responses, it is reasonable to propose that regulation of FBW7 expression may alleviate antibody-mediated autoimmune diseases. In the present study, we showed that FBW7 is a crucial exacerbating factor for disease development and progression in the CIA mouse model. Our results showed that, in the pathological state, FBW7 deletion ameliorated the incidence and severity of CIA by decreasing the generation of anti-CII antibodies. Although antibody titres were measured at the end point of the disease in mice, levels of CII-specific antibody levels in the experimental group were still lower than in the control group. The development of CIA depends on the effective priming of humoral responses for producing arthritogenic CII-specific IgG autoantibodies in GCs [86–88]. Recently, several reports have highlighted the role of FBW7 in regulating proinflammatory signalling [89], and in innate immunity and related diseases [32, 34–36]. Our study sheds more light on the role of FBW7 in B-cell-mediated autoimmune disease, providing for novel approaches and theoretical rationales for understanding the pathogenesis of CIA or RA. More questions still need to be answered before translation can be considered. Unlike CIA, clinical RA is complex and heterogeneous. The association between FBW7 and RA disease needs to be verified by more clinical data and more detailed basic studies.

In conclusion, our evaluation of mice lacking FBW7 specifically in B-cell compartments has identified a requirement for this molecule in B-cell antibody responses and in the pathogenesis of experimental autoimmune

arthritis. FBW7 is important for the maintenance of mature B and B1 B cells, and it is indispensable for the proliferation and survival of B cells in response to BCR signalling. Our results emphasize a critical function of FBW7 in B cell-mediated germinal centre responses. Genetic ablation of FBW7 at the GC B stage led to suppressed Ig class-switching and diminished antibody affinity maturation. Moreover, our work showed that FBW7 conditionally knocked out at the GC B stage ameliorated the pathogenesis in the autoimmune disease model of collagen-induced arthritis, indicating potential application of specific FBW7 inhibitors for treating RA and potentially other GC-associated and autoantibody-driven autoimmune diseases. In general, these findings further our understanding of germinal centre biology and autoimmune arthritis.

ACKNOWLEDGEMENTS

We thank EditSprings (https://www.editsprings. com/) for the expert linguistic services provided.

CONFLICT OF INTEREST

The authors declare that they have no conflicts of interest with the contents of this article.

AUTHOR CONTRIBUTIONS

Chunlei Feng involved in investigation, methodology and visualization and wrote original draft. Lingyun Li performed validation and formal analysis. Lei Zhou reviewed and edited the article. Dali Li and Mingyao Liu performed resources. Shuhua Han involved in project administration. Biao Zheng involved in conceptualization and supervision, and reviewed and edited the document.

ORCID

Biao Zheng https://orcid.org/0000-0002-0216-1022

REFERENCES

1. Cooper MD. The early history of B cells. Nat Rev Immunol. 2015;15:191–7.
2. Hardy RR, Hayakawa K. B cell development pathways. Annu Rev Immunol. 2001;19:595–621.
3. Ichii M, Oritani K, Kanakura Y. Early B lymphocyte development: similarities and differences in human and mouse. World J Stem Cells. 2014;6:421–31.
4. Hsu MC, Toellner KM, Vinuesa CG, Maclennan IC. B cell clones that sustain long-term plasmablast growth in T-independent extrafollicular antibody responses. Proc Natl Acad Sci USA. 2006;103:5905–10.
5. MacLennan IC, Toellner KM, Cunningham AF, Serre K, Sze DM, Zuniga E, et al. Extrafollicular antibody responses. Immunol Rev. 2003;194:8–18.
6. Elsner RA, Shlomchik MJ. Germinal center and extrafollicular B cell responses in vaccination, immunity, and autoimmunity. Immunity. 2020;53:1136–50.
7. Huang C. Germinal center reaction. Adv Exp Med Biol. 2020;1254:47–53.
8. Fagarasan S, Honjo T. T-Independent immune response: new aspects of B cell biology. Science. 2000;290:89–92.
9. Martin F, Oliver AM, Kearney JF. Marginal zone and B1 B cells unite in the early response against T-independent blood-borne particulate antigens. Immunity. 2001;14:617–29.
10. Balazs M, Martin F, Zhou T, Kearney J. Blood dendritic cells interact with splenic marginal zone B cells to initiate T-independent immune responses. Immunity. 2002;17:341–52.
11. McHeyzer-Williams MG. B cells as effectors. Curr Opin Immunol. 2003;15:354–61.
12. Victora GD, Nussenzweig MC. Germinal centers. Annu Rev Immunol. 2012;30:429–57.
13. Shlomchik MJ, Weisel F. Germinal centers. Immunol Rev. 2012;247:5–10.
14. Gars E, Butzmann A, Ohgami R, Balakrishna JP, O'Malley DP. The life and death of the germinal center. Ann Diagn Pathol. 2020;44:151421.
15. Chandra V, Bortnick A, Murre C. AID targeting: old mysteries and new challenges. Trends Immunol. 2015;36:527–35.
16. Vinuesa CG, Sanz I, Cook MC. Dysregulation of germinal centres in autoimmune disease. Nat Rev Immunol. 2009;9:845–57.
17. Schroder AE, Greiner A, Seyfert C, Berek C. Differentiation of B cells in the nonlymphoid tissue of the synovial membrane of patients with rheumatoid arthritis. Proc Natl Acad Sci USA. 1996;93:221–5.
18. Pitzalis C, Jones GW, Bombardieri M, Jones SA. Ectopic lymphoid-like structures in infection, cancer and autoimmunity. Nat Rev Immunol. 2014;14:447–62.
19. Edwards JCW, Cambridge G. Prospects for B-cell-targeted therapy in autoimmune disease. Rheumatology. 2005;44:151–6.
20. Nakken B, Munthe LA, Konttinen YT, Sandberg AK, Szekanecz Z, Alex P, et al. B-cells and their targeting in rheumatoid arthritis - Current concepts and future perspectives. Autoimmun Rev. 2011;11:28–34.
21. Yildirim-Toruner C, Diamond B. Current and novel therapeutics in the treatment of systemic lupus erythematosus. J Allergy Clin Immun. 2011;127:303–12.
22. Lino A. Post-activated B cells in autoimmunity. Ann Rheum Dis. 2019;78:24–5.
23. Leandro M. B cells and rheumatoid factors in autoimmunity. Int J Rheum Dis. 2015;18:379–81.
24. Dorner T, Giesecke C, Lipsky PE. Mechanisms of B cell autoimmunity in SLE. Arthritis Res Ther. 2011;13:243.
25. Brand DD, Latham KA, Rosloniec EF. Collagen-induced arthritis. Nat Protoc. 2007;2:1269–75.
26. Williams RO. Collagen-induced arthritis in mice. Methods Mol Med. 2007;136:191–9.
27. Yanaba K, Hamaguchi Y, Venturi GM, Steeber DA, St Clair EW, Tedder TF. B cell depletion delays collagen-induced arthritis in mice: arthritis induction requires synergy between humoral and cell-mediated immunity. J Immunol. 2007;179:1369–80.
28. Han SH, Cao ST, Bheekha-Escura R, Zheng B. Germinal center reaction in the joints of mice with collagen-induced arthritis - An animal model of lymphocyte activation and differentiation in arthritic joints. Arthritis Rheum. 2001;44:1438–43.
29. Yumimoto K, Nakayama KI. Recent insight into the role of FBXW7 as a tumor suppressor. Semin Cancer Biol. 2020; 67(Pt 2):1–15.

30. Davis RJ, Welcker M, Clurman BE. Tumor suppression by the Fbw7 ubiquitin ligase: mechanisms and opportunities. Cancer Cell. 2014;26:455–64.
31. Welcker M, Clurman BE. FBW7 ubiquitin ligase: a tumour suppressor at the crossroads of cell division, growth and differentiation. Nat Rev Cancer. 2008;8:83–93.
32. Wang C, Chao Y, Xu W, Liu Z, Wang H, Huang K. Myeloid FBW7 deficiency disrupts redox homeostasis and aggravates dietary-induced insulin resistance. Redox Biol. 2020;37:101688.
33. Song Y, Lai L, Chong Z, He J, Zhang Y, Xue Y, et al. E3 ligase FBXW7 is critical for RIG-I stabilization during antiviral responses. Nat Commun. 2017;8:14654.
34. Chong Z, Bao C, He J, Chen T, Zhong L, Li G, et al. E3 ligase FBXW7 aggravates TMPD-induced systemic lupus erythematosus by promoting cell apoptosis. Cell Mol Immunol. 2018;15:1057–70.
35. He J, Song Y, Li G, Xiao P, Liu Y, Xue Y, et al. Fbxw7 increases CCL2/7 in CX3CR1hi macrophages to promote intestinal inflammation. J Clin Invest. 2019;129:3877–93.
36. Meng Q, Wu W, Pei T, Xue J, Xiao P, Sun L, et al. miRNA-129/FBW7/NF-kappaB, a novel regulatory pathway in inflammatory bowel disease. Mol Ther Nucleic Acids. 2020;19:731–40.
37. Matsuoka S, Oike Y, Onoyama I, Iwama A, Arai F, Takubo K, et al. Fbxw7 acts as a critical fail-safe against premature loss of hematopoietic stem cells and development of T-ALL. Genes Dev. 2008;22:986–91.
38. Thompson BJ, Jankovic V, Gao J, Buonamici S, Vest A, Lee JM, et al. Control of hematopoietic stem cell quiescence by the E3 ubiquitin ligase Fbw7. J Exp Med. 2008;205:1395–408.
39. Ramezani-Rad P, Leung CR, Apgar JR, Rickert RC. E3 ubiquitin ligase Fbw7 regulates the survival of mature B cells. J Immunol. 2020;204:1535–42.
40. Assadian F, Sandstrom K, Laurell G, Svensson C, Akusjarvi G, Punga T. Efficient isolation protocol for B and T lymphocytes from human palatine tonsils. J Vis Exp. 2015;105:53374.
41. Campbell IK, Hamilton JA, Wicks IP. Collagen-induced arthritis in C57BL/6 (H-2b) mice: new insights into an important disease model of rheumatoid arthritis. Eur J Immunol. 2000;30:1568–75.
42. Jacob J, Kelsoe G. In situ studies of the primary immune response to (4-hydroxy-3-nitrophenyl)acetyl. II. A common clonal origin for periarteriolar lymphoid sheath-associated foci and germinal centers. J Exp Med. 1992;176:679–87.
43. Han S, Marinova E, Zheng B. Rectification of age-related impairment in Ig gene hypermutation during a memory response. Int Immunol. 2004;16:525–32.
44. Rickert RC, Roes J, Rajewsky K. B lymphocyte-specific, Cre-mediated mutagenesis in mice. Nucleic Acids Res. 1997;25:1317–8.
45. Smith FI, Tesch H, Rajewsky K. Heterogeneous and monoclonal helper T cells induce similar anti-(4-hydroxy-3-nitrophenyl) acetyl (NP) antibody populations in the primary adoptive response. II. Lambda light chain dominance and idiotope expression. Eur J Immunol. 1984;14:195–200.
46. Jacob J, Kassir R, Kelsoe G. In situ studies of the primary immune response to (4-hydroxy-3-nitrophenyl)acetyl. I. The architecture and dynamics of responding cell populations. J Exp Med. 1991;173:1165–75.
47. Garcia de Vinuesa C, O'Leary P, Sze DM, Toellner KM, MacLennan IC. T-independent type 2 antigens induce B cell proliferation in multiple splenic sites, but exponential growth is confined to extrafollicular foci. Eur J Immunol. 1999;29:1314–23.
48. Shih TA, Roederer M, Nussenzweig MC. Role of antigen receptor affinity in T cell-independent antibody responses in vivo. Nat Immunol. 2002;3:399–406.
49. Ju ST, Dorf ME. Preferential induction of specific lambda-isotypic antibodies in mice. J Immunol. 1984;133:1404–9.
50. Mongini PK, Longo DL, Paul WE. T cell regulation of immunoglobulin class expression in the B cell response to TNP-Ficoll: characterization of the T cell responsible for preferential enhancement of the IgG2a response. J Immunol. 1984;132:1647–53.
51. Casola S, Cattoretti G, Uyttersprot N, Koralov SB, Seagal J, Hao Z, et al. Tracking germinal center B cells expressing germ-line immunoglobulin gamma1 transcripts by conditional gene targeting. Proc Natl Acad Sci USA. 2006;103:7396–401.
52. Jacob J, Przylepa J, Miller C, Kelsoe G. In situ studies of the primary immune response to (4-hydroxy-3-nitrophenyl)acetyl. III. The kinetics of V region mutation and selection in germinal center B cells. J Exp Med. 1993;178:1293–307.
53. Jacob J, Kelsoe G, Rajewsky K, Weiss U. Intraclonal generation of antibody mutants in germinal centres. Nature. 1991;354:389–92.
54. Allen D, Simon T, Sablitzky F, Rajewsky K, Cumano A. Antibody engineering for the analysis of affinity maturation of an anti-hapten response. EMBO J. 1988;7:1995–2001.
55. Cariappa A, Mazo IB, Chase C, Shi HN, Liu H, Li Q, et al. Perisinusoidal B cells in the bone marrow participate in T-independent responses to blood-borne microbes. Immunity. 2005;23:397–407.
56. Pillai S, Cariappa A. The follicular versus marginal zone B lymphocyte cell fate decision. Nat Rev Immunol. 2009;9:767–77.
57. Baumgarth N. The double life of a B-1 cell: self-reactivity selects for protective effector functions. Nat Rev Immunol. 2011;11:34–46.
58. Casola S, Otipoby KL, Alimzhanov M, Humme S, Uyttersprot N, Kutok JL, et al. B cell receptor signal strength determines B cell fate. Nat Immunol. 2004;5:317–27.
59. Maizels N, Bothwell A. The T-cell-independent immune response to the hapten NP uses a large repertoire of heavy chain genes. Cell. 1985;43(3 Pt 2):715–20.
60. Chan TD, Gatto D, Wood K, Camidge T, Basten A, Brink R. Antigen affinity controls rapid T-dependent antibody production by driving the expansion rather than the differentiation or extrafollicular migration of early plasmablasts. J Immunol. 2009;183:3139–49.
61. Horwitz BH, Zelazowski P, Shen Y, Wolcott KM, Scott ML, Baltimore D, et al. The p65 subunit of NF-kappa B is redundant with p50 during B cell proliferative responses, and is required for germline CH transcription and class switching to IgG3. J Immunol. 1999;162:1941–6.
62. Hodgkin PD, Lee JH, Lyons AB. B cell differentiation and isotype switching is related to division cycle number. J Exp Med. 1996;184:277–81.
63. Chi X, Li Y, Qiu X. V(D)J recombination, somatic hypermutation and class switch recombination of immunoglobulins: mechanism and regulation. Immunology. 2020;160:233–47.
64. Muramatsu M, Kinoshita K, Fagarasan S, Yamada S, Shinkai Y, Honjo T. Class switch recombination and hypermutation

require activation-induced cytidine deaminase (AID), a potential RNA editing enzyme. Cell. 2000;102:553–63.
65. Dominguez-Sola D, Kung J, Holmes AB, Wells VA, Mo T, Basso K, et al. The FOXO1 transcription factor instructs the germinal center dark zone program. Immunity. 2015;43:1064–74.
66. Inoue T, Shinnakasu R, Ise W, Kawai C, Egawa T, Kurosaki T. The transcription factor Foxo1 controls germinal center B cell proliferation in response to T cell help. J Exp Med. 2017;214:1181–98.
67. Sander S, Chu VT, Yasuda T, Franklin A, Graf R, Calado DP, et al. PI3 kinase and FOXO1 transcription factor activity differentially control B cells in the germinal center light and dark zones. Immunity. 2015;43:1075–86.
68. Klein U, Casola S, Cattoretti G, Shen Q, Lia M, Mo T, et al. Transcription factor IRF4 controls plasma cell differentiation and class-switch recombination. Nat Immunol. 2006;7:773–82.
69. Ochiai K, Maienschein-Cline M, Simonetti G, Chen J, Rosenthal R, Brink R, et al. Transcriptional regulation of germinal center B and plasma cell fates by dynamical control of IRF4. Immunity. 2013;38:918–29.
70. Sciammas R, Shaffer AL, Schatz JH, Zhao H, Staudt LM, Singh H. Graded expression of interferon regulatory factor-4 coordinates isotype switching with plasma cell differentiation. Immunity. 2006;25:225–36.
71. Hauser J, Grundstrom C, Kumar R, Grundstrom T. Regulated localization of an AID complex with E2A, PAX5 and IRF4 at the Igh locus. Mol Immunol. 2016;80:78–90.
72. Crotty S, Johnston RJ, Schoenberger SP. Effectors and memories: Bcl-6 and Blimp-1 in T and B lymphocyte differentiation. Nat Immunol. 2010;11:114–20.
73. Yeh CH, Bellon M, Nicot C. FBXW7: a critical tumor suppressor of human cancers. Mol Cancer. 2018;17:115.
74. Song S, Matthias PD. The transcriptional regulation of germinal center formation. Front Immunol. 2018;9:2026.
75. Dominguez-Sola D, Victora GD, Ying CY, Phan RT, Saito M, Nussenzweig MC, et al. The proto-oncogene MYC is required for selection in the germinal center and cyclic reentry. Nat Immunol. 2012;13:1083–91.
76. Calado DP, Sasaki Y, Godinho SA, Pellerin A, Kochert K, Sleckman BP, et al. The cell-cycle regulator c-Myc is essential for the formation and maintenance of germinal centers. Nat Immunol. 2012;13:1092–100.
77. Vikstrom I, Carotta S, Luthje K, Peperzak V, Jost PJ, Glaser S, et al. Mcl-1 is essential for germinal center formation and B cell memory. Science. 2010;330:1095–9.
78. Ding C, Chen X, Dascani P, Hu X, Bolli R, Zhang HG, et al. STAT3 signaling in B cells is critical for germinal center maintenance and contributes to the pathogenesis of murine models of lupus. J Immunol. 2016;196:4477–86.
79. Yao S, Xu F, Chen Y, Ge Y, Zhang F, Huang H, et al. Fbw7 regulates apoptosis in activated B-cell like diffuse large B-cell lymphoma by targeting Stat3 for ubiquitylation and degradation. J Exp Clin Cancer Res. 2017;36:10.
80. Chen Y, Sun XX, Sears RC, Dai MS. Writing and erasing MYC ubiquitination and SUMOylation. Genes Dis. 2019;6:359–71.
81. Lee J, Park H, Lim J, Jin HS, Park Y, Jung YJ, et al. GSK3 restrains germinal center B cells to form plasma cells. J Immunol. 2021;206:481–93.
82. Smolen JS, Aletaha D, McInnes IB. Rheumatoid arthritis. Lancet. 2016;388:2023–38.
83. Suurmond J, Diamond B. Autoantibodies in systemic autoimmune diseases: specificity and pathogenicity. J Clin Invest. 2015;125:2194–202.
84. Willemze A, Trouw LA, Toes RE, Huizinga TW. The influence of ACPA status and characteristics on the course of RA. Nat Rev Rheumatol. 2012;8:144–52.
85. Huang H, Benoist C, Mathis D. Rituximab specifically depletes short-lived autoreactive plasma cells in a mouse model of inflammatory arthritis. Proc Natl Acad Sci USA. 2010;107:4658–63.
86. Svensson L, Jirholt J, Holmdahl R, Jansson L. B cell-deficient mice do not develop type II collagen-induced arthritis (CIA). Clin Exp Immunol. 1998;111:521–6.
87. Dahdah A, Habir K, Nandakumar KS, Saxena A, Xu B, Holmdahl R, et al. Germinal center B cells are essential for collagen-induced arthritis. Arthritis Rheumatol. 2018;70:193–203.
88. Corthay A, Johansson A, Vestberg M, Holmdahl R. Collagen-induced arthritis development requires alpha beta T cells but not gamma delta T cells: studies with T cell-deficient (TCR mutant) mice. Int Immunol. 1999;11:1065–73.
89. Balamurugan K, Sharan S, Klarmann KD, Zhang Y, Coppola V, Summers GH, et al. FBXW7alpha attenuates inflammatory signalling by downregulating C/EBPdelta and its target gene Tlr4. Nat Commun. 2013;4:1662.

SUPPORTING INFORMATION

Additional supporting information may be found online in the Supporting Information section.

How to cite this article: Feng C, Li L, Zhou L, Li D, Liu M, Han S, et al. Critical roles of the E3 ubiquitin ligase FBW7 in B-cell response and the pathogenesis of experimental autoimmune arthritis. Immunology. 2021;164:617–636. https://doi.org/10.1111/imm.13398